Canada - France
Pipeline - Ground Freezing Experiment:
Phase VIII

Fourth Freeze Cycle

Geotechnical Science Laboratories
Carleton University
Ottawa, Ontario
K1S 5B6

Report to Permafrost Section,
Terrain Sciences Division,
Geological Survey of Canada,
Energy, Mines and Resources Canada

July 1988

Forward

This report describes findings from the fourth freeze cycle of the Canada-France pipeline ground freezing project. It describes activities over the contract period April 1 1988 to March 30 1989.

New equipment installed at the end of the third cycle has functioned well and the observations have confirmed and added to the picture being obtained of the origin of the freezing-induced stresses in the soil which give rise to pipe deformation.

During the contract period, there was considerable interest in the work and in the earlier reports, on the part of consultants and pipeline and petroleum companies. Data were prepared and supplied on discs to a consultant concerned with field detection of pipeline deflections. Also during the contract period, detailed discussions were initiated with companies concerned with the reactivated proposals for bringing gas by pipeline down the Mackenzie Valley. It now appears that, following a further short phase with the existing experimental configuration, there will be a major renewal of the project with joint industry/government funding. This will allow a number of important unresolved issues, relating to northern pipelines in practice and which have come to light during the experiment, to be fully investigated. The development will also be a highly significant example of the cooperation of industry, government and research institutions (including the university component),

from two countries, to find solutions to scientific problems having a direct industrial significance.

The essential role of our French colleagues is again acknowledged. During the contract period a seminar was given in Ottawa by Michel Fremond on the advanced mathematical modelling procedures he and his associates have developed. The models now encompass the thermal, hydrologic, and mechanical aspects (stress fields) of the freezing soil. The Project was also described at the France-Canada workshop held in Paris and organised by the Department of External Affairs (Ottawa) and the Ministere des Affaires Etrangeres in France.

Since commencement of the experiment in 1982, reports similar in format to the present one have been prepared annually and occasionally more frequently. A number of copies of each report have been purchased by companies and others with a specific interest in the topic. Twelve papers have been published in journals or conference proceedings. A further seven papers have been published which relate to aspects of the study, but the work for which has been funded from other sources. A number of more general or 'popular' accounts have also appeared in various publications. Several graduate student theses have pertained to the work.

The present report was prepared by D. E. Patterson and D. Riseborough, joint Project Managers, Ottawa, with contributions by Dr. M. W. Smith and Dr. P. J. Williams, Co-Principal Investigators. Appendix I was prepared by M. Shen and B. Ladanyi, CINEP, Ecole Polytechnique de Montreal.

The Canada-France project comprises a team of Canadian and French scientists, engineers, technicians and graduate students. The on-site assistance of M.A. Dupas and M.B. Dumoulin are particularly noted, and the smooth cooperation with Laboratoire Central des Ponts et Chaussees and the Centre de Geomorphologie of the CNRS is of fundamental importance to the project. The project as a whole is supervised by a scientific committee. The members and their affiliations are listed below.

M. Jaime Aguirre-Puente, Laboratoire d'Aerothermique, Centre National de la Recherche Scientifique

M. J-P. Lautridou, Centre National de la Recherche Scientifique

* M. Michel Fremond, Laboratoire Central des Ponts et Chauss es

Dr. A. Judge, Earth Physics Branch, Energy, Mines and Resources, Canada

M. Chantereau, Laboratoire Central des Ponts et Chauss es

M.S. Philippe, Laboratoire Central des Ponts et Chauss es

Dr. M.W. Smith, Geotechnical Science Laboratories, Carleton University

** Dr. P.J. Williams, Geotechnical Science Laboratories, Carleton University

* chairman France
** chairman Canada

Table of Contents

1 Introduction 1
1.1 Scope of this Report 1

2 Operational Conditions and Instrument Locations for the Fourth Freeze Cycle 2
2.1 General conditions 2
2.2 Instrument and Site Locations 2
2.2.1 Soil Heave and Temperature 2
2.2.2 Surface Heave 4
2.2.3 Pipe Deflection 4
2.2.4 Pressure Measurements 4
2.2.5 Pipe Stress 8
2.3 Instrumentation for the Fifth Freeze Cycle 9

3 Observations During the Fourth Freeze Cycle 10
3.1 General 10
3.2 Thermal Conditions 10
3.3 Total Heave at Magnet Heave Sites 14
3.4 Differential Strain at the Magnet Heave Sites . . . 22
3.5 Pipe displacement 33
3.6 Pipe stress 33
3.7 Soil Pressures 39
3.7.1 Petur Cells 39
3.7.2 Glotzl Cells 49
3.9 Surface Levelling 53
3.9.1 Surface changes between cycles. 54
3.9.2 Total Heave during the fourth freeze cycle. . 56
3.9.3 Heave rates over time. 58

References 62

Appendix I

Use of boundary-fitted Curvilinear Coordinate Systems in connection with chilled pipeline design. 64

Appendix II

Density-Water Content Profiles 73

1 Introduction

1.1 Scope of this Report

This report examines the observations made during the fourth freeze cycle of this project. Particular attention is given to the heave observations (differential and surface) and the density profiles obtained towards the end of this cycle.

The timetable of events to date is shown in Table 1.1.

Table 1.1 Timetable of Events

Event	Date from	Date to	Operating Conditions Air/Ground temp. (C)	Operating Conditions Pipe temp. (C)
First Freeze	09/21/82	08/06/83	-0.75	-2.0
Surface Thaw	08/06/83	17/10/83	4.0	-2.0
Second Freeze	17/10/83	18/09/85	-0.75	-5.0
Second Thaw	18/09/85	01/02/86	4.0	ambient
Re-instru-mentation	01/02/86	03/03/86	-	-
Third Freeze	03/03/86	25/02/87	-0.75	-5.25
Third Thaw	25/02/87	21/05/87	4.0	ambient
Shutdown	21/05/87	06/01/88	-	-
Fourth Freeze	06/01/88	24/05/89	-0.75	-5.25

2 Operational Conditions and Instrument Locations for the Fourth Freeze Cycle

2.1 General conditions

The temperature conditions for this freeze cycle are the same as those used during the second and third cycles. The compressors controlling air and pipe temperature are still maintained at approximately -0.75 and -5.25 C respectively. The water table is maintained at 90 cm beneath the soil surface, as in the past.

2.2 Instrument and Site Locations

2.2.1 Soil Heave and Temperature

Soil heave and temperature, since the third freeze cycle, have been determined at specific sites in order to better characterize their spatial and temporal variability. Total heave and differential strain are determined using the magnet heave device (Geotechnical Science Laboratories 1988 and Smith and Patterson 1989). A companion thermistor string is located in close proximity to each magnet heave site to assist in assessing the thermal conditions during freezing.

The sites where soil heave and temperature measurements are made are given in Table 2.1. Sites 1 to 9 are in the silt section of the facility while site 10 is in the sand. The **along axis** column refers to the distance of the site relative to the sand-silt and the **off axis** column denotes the site's proximity to the pipe axis.

Table 2.1 <u>Heave and Temperature Sensor Locations</u>

	Heave Sites		Temperature Sites	
Site No.	Distance along axis (cm)	Distance off axis (cm)	Distance along axis (cm)	Distance off axis (cm)
1	540.0	23.5	555.5	23.5
2	429.0	27.0	438.5	25.0
3	427.5	65.5	439.0	63.5
4	434.0	102.5	444.0	100.5
5	421.5	201.0	433.0	200.0
6	318.0	25.0	328.0	25.0
7	203.5	28.0	216.5	28.0
8	102.5	26.5	124.5	27.0
9	53.0	26.0	63.0	23.5
10	-49.0	25.0	-62.0	25.0

Sites 1-9 in silt section

2.2.2 Surface Heave

Heave of the soil surface is measured via optical levelling at various locations within the facility. A grid of locations can be constructed with measurement sites located at -3.0, -2.0, -1.5, -1.0, -0.5, 0.0, 0.5, 1.0, 1.5, 2.0, and 3.0 m normal to the pipe axis (negative numbers refer to the right side of the pipe axis while observing the facility from the instrument room) and -7.0, -6.0, -5.0, -4.5, -4.0, -3.0, -2.0, -1.0, -0.5, 0.0, 0.5, 1.0, 2.0, 3.0, 4.0, 4.5, 5.0, 6.0 and 7.0 m parallel to the pipe axis (negative numbers are sites located in the silt section of the facility). Position 0,0 is on the pipe axis at the sand-silt transition.

2.2.3 Pipe Deflection

Pipe shape has been determined since the first freeze cycle by optically levelling a series or rods attached to the pipe. The location of these rods is given in Table 2.2

2.2.4 Pressure Measurements

Soil stress is determined with an array of Petur cells and Glotzl cells. The Petur cells are much smaller than the Glotzl and they are designed to measure either total or directional pressures being exerted during soil freezing.

The Petur cells were refurbished before the commencement of this freeze cycle to correct design deficiencies. There are five

arrays of Petur cells installed at various locations. Their location within the facility is outlined in Table 2.3. The type of cell is also indicated with a t for total pressure, a v for cells measuring the vertical component and an l for cells measuring the lateral component.

The Glotzl cells have been in position since the first freeze cycle at various locations along the pipe axis. The placement depth for these cells is with respect to the bottom of the pipe. The location of the various sensors is given in Table 2.4.

Table 2.2 Location of Rods on Pipe to Determine Pipe Shape

Silt Section		Sand Section	
Number	Distance from sand-silt transition	Number	Distance from sand-silt transition
1	-7.37	15	0.00
2	-6.20	16	0.30
3	-5.70	17	0.80
4	-5.20	18	1.30
5	-4.70	19	1.80
6	-4.20	20	2.30
7	-3.70	21	2.80
8	-3.20	22	3.30
9	-2.70	23	3.80
10	-2.20	24	4.30
11	-1.70	25	4.80
12	-1.20	26	5.30
13	-0.70	27	5.80
14	-0.20	28	6.30
		29	7.36

Table 2.3 Location of Petur Cells

Site #	Cell #	Distance from transition	Distance from Pipe	Depth	Type
1	1	4.00	0.00	0.80	t
	2	4.15	0.00	1.01	v
	3	4.00	0.00	1.01	t
	4	3.85	0.00	1.01	l
	5	4.00	0.00	1.18	t
	6	4.00	0.00	1.40	t
2	7	3.66	1.03	0.45	t
	8	3.66	1.03	0.75	t
	9	3.66	1.03	1.05	t
	10	3.66	1.03	1.35	t
3	11	2.35	0.00	0.10*	t
	12	2.35	0.00	0.30*	t
4	13	0.85	0.00	0.80	t
	14	1.00	0.00	1.01	v
	15	0.85	0.00	1.01	t
	16	0.70	0.00	1.01	l
	17	0.85	0.00	1.18	t
	18	0.85	0.00	1.40	t
5	19	-2.35	0.00	0.10*	t
	20	-2.35	0.00	0.30*	t

t total pressure
v directional (vertical component)
l directional (lateral component)

Sites 1 to 4 are in the silt section and site 5 is in the sand.

All distances are in metres from the sand-silt transition and all depths are in metres beneath the soil surface except those noted below.

Depths marked with a * denote sensors located beneath the cavity which has formed between the pipe and the soil. The depths noted are beneath this cavity.

Table 2.4 Location of Glotzl Cells

Cell #	Distance from transition	Distance from Pipe	Depth Beneath Pipe
1	7.00	0.00	0.46
2	4.50	0.00	0.86
3	4.50	0.00	0.46
4	4.50	0.00	0.10
5	4.50	0.25	0.46
6	4.50	1.00	0.00
7	2.00	0.00	0.46
8	-2.00	0.00	0.46
9	-4.50	0.00	0.86
10	-4.50	0.00	0.46
11	-4.50	0.00	0.10
12	-4.50	0.25	0.46
13	-4.50	1.00	0.00
14	-7.00	0.00	0.46

Cells 1 to 7 are in the silt section and cells 8 to 14 are in the sand.

All distances are in metres from the sand-silt transition and all depths are in metres beneath the pipe.

Cells 5, 6, 12 and 13 are installed in a vertical orientation to measure lateral pressures.

2.2.5 Pipe Stress

Strain gauges were mounted on the pipe at various locations prior to the first freeze. Several of these gauges have since ceased to function and will need to be replaced when a complete refurbishment of the facility is undertaken. The initial placement of the gauges is given in Table 2.5.

Table 2.5 Strain Gauge Locations

Sensor	Distance from transition	Sensor	Distance from transition
1	7.05	12	0.14
2	5.62	13	0.54
3	4.33	14	0.90
4	3.59	15	1.24
5	3.00	16	1.60
6	2.33	17	2.34
7	1.49	18	3.05
8	1.09	19	3.64
9	0.79	20	4.40
10	0.48	21	5.68
11	0.09	22	7.13

All distances in metres

2.3 Instrumentation for the Fifth Freeze Cycle

The choice and placement of instrumentation for the fifth freeze cycle is still being considered and may depend upon the overall experimental design. It is clear though, that heave measurements (total and differential) will continue to be made. It is probable that a more extensive network of magnet heave sensors will be installed to more fully characterize the spatial variability of heave and strain.

Also, there are difficulties in determining the position of certain sensors over time because of soil heave. A number of sensors, such as the Glotzl cells, Petur cells and thermistors are referred to by their initial placement. In order to determine a sensor's depth relative to the soil surface at a given point in time, the position of the frost line and the amount of heave need to be known at that point. In most instances, this is not known with any certainty nor can it be easily determined. Sensors which cannot be placed at a fixed depth relative to the soil surface will need to be located close to magnet heave and thermistor sites to permit better depth referencing.

3 Observations During the Fourth Freeze Cycle

3.1 General

This section concentrates largely on the heave/differential strain characteristics observed with the magnet heave device as well as the spatial and temporal variations of surface heave as observed from optical levelling. A discussion of the soil pressure measurements is also given.

3.2 Thermal Conditions

Figure 3.1 shows the position of the 0 C isotherm for selected dates. In general, the 0 C isotherm position parallels the pipe position for all sites within 1 m of the transition (thermistor sites 1, 2, 6, 7 and 8). The 0 C isotherm position deepens as the transition is approached (thermistor sites 9 and 10).

Figure 3.2 shows the 0 C isotherm position over time. Site 8 is used to represent locations not influenced by the thermal conditions induced by the soil transition. Site 9 is 50 cm from the transition in the silt and site 10 is 50 cm from the transition in the sand. The patterns are similar to those found during the third freeze. One should note that the effect of the compressor shut-down on day 230 is evident at all three sites.

Figure 3.3 shows the 0 C isotherm position for selected dates in the silt near the BB cross-section (4.4 m from the sand-silt transition). As is shown, proximity to the pipe greatly affects soil freezing. At about 2 m from the pipe axis, freezing is controlled by ambient conditions (-0.75 C).

Figure 3.1

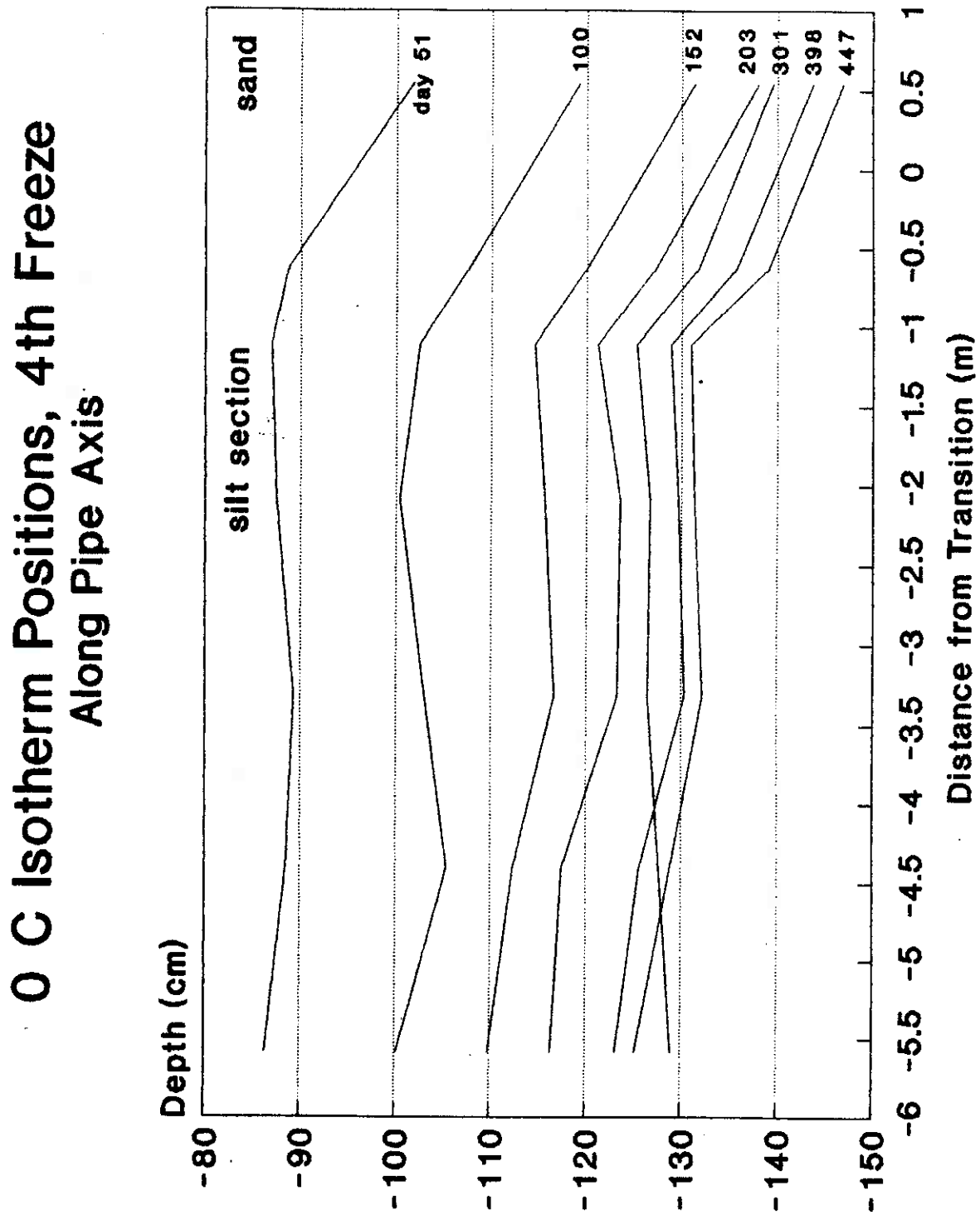
0 C Isotherm Positions, 4th Freeze
Along Pipe Axis
Depth (cm)
-80
-90
-100
-110
-120
-130
-140
-150
silt section
sand
day 51
100
152
203
301
398
447
-6
-5.5
-5
-4.5
-4
-3.5
-3
-2.5
-2
-1.5
-1
-0.5
0
0.5
1
Distance from Transition (m)

Figure 3.2

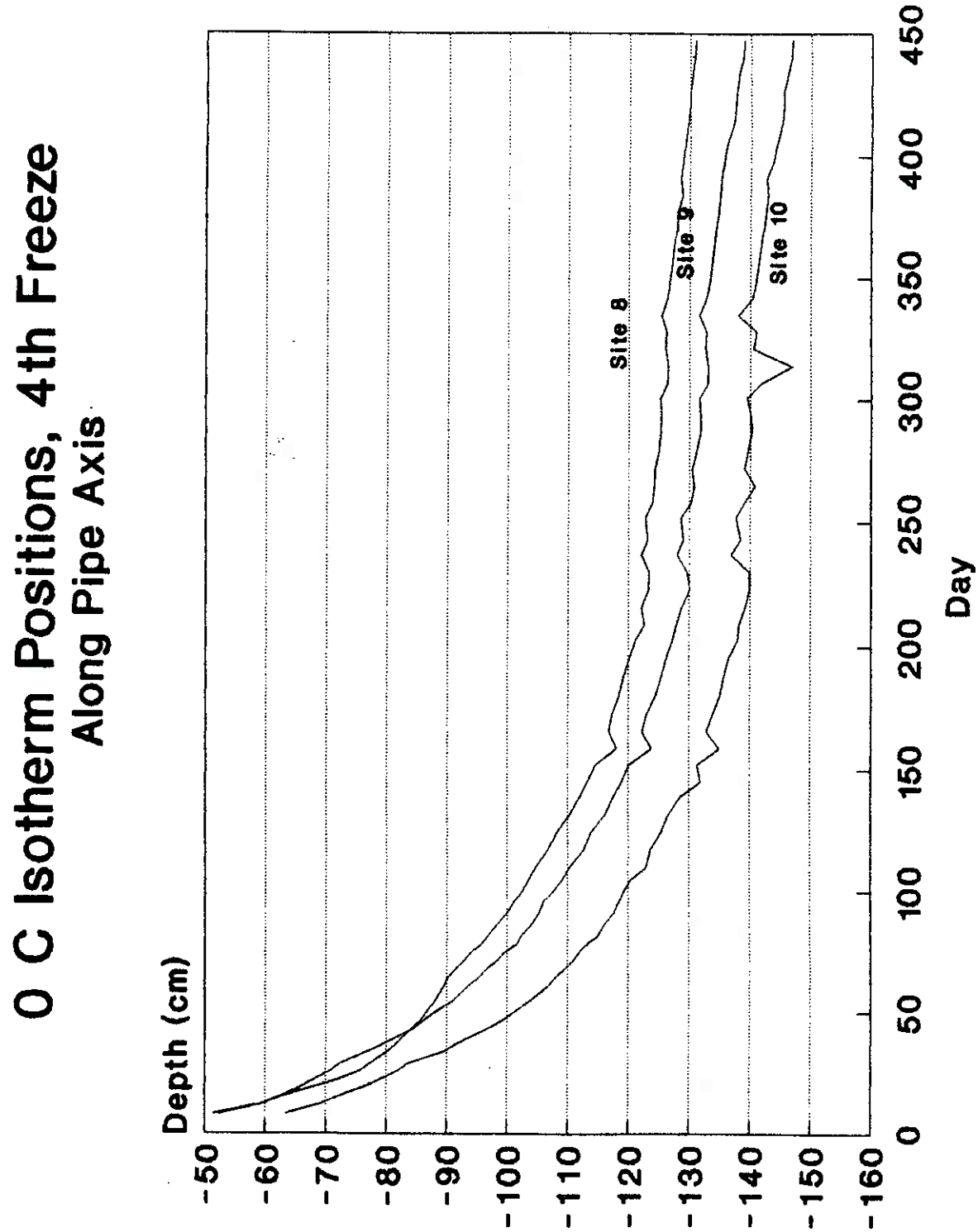
0 C Isotherm Positions, 4th Freeze
Along Pipe Axis
Depth (cm)
-50
-60
-70
-80
-90
-100
-110
-120
-130
-140
-150
-160
0
50
100
150
200
250
300
350
400
450
Day
Site 8
Site 9
Site 10

Figure 3.3

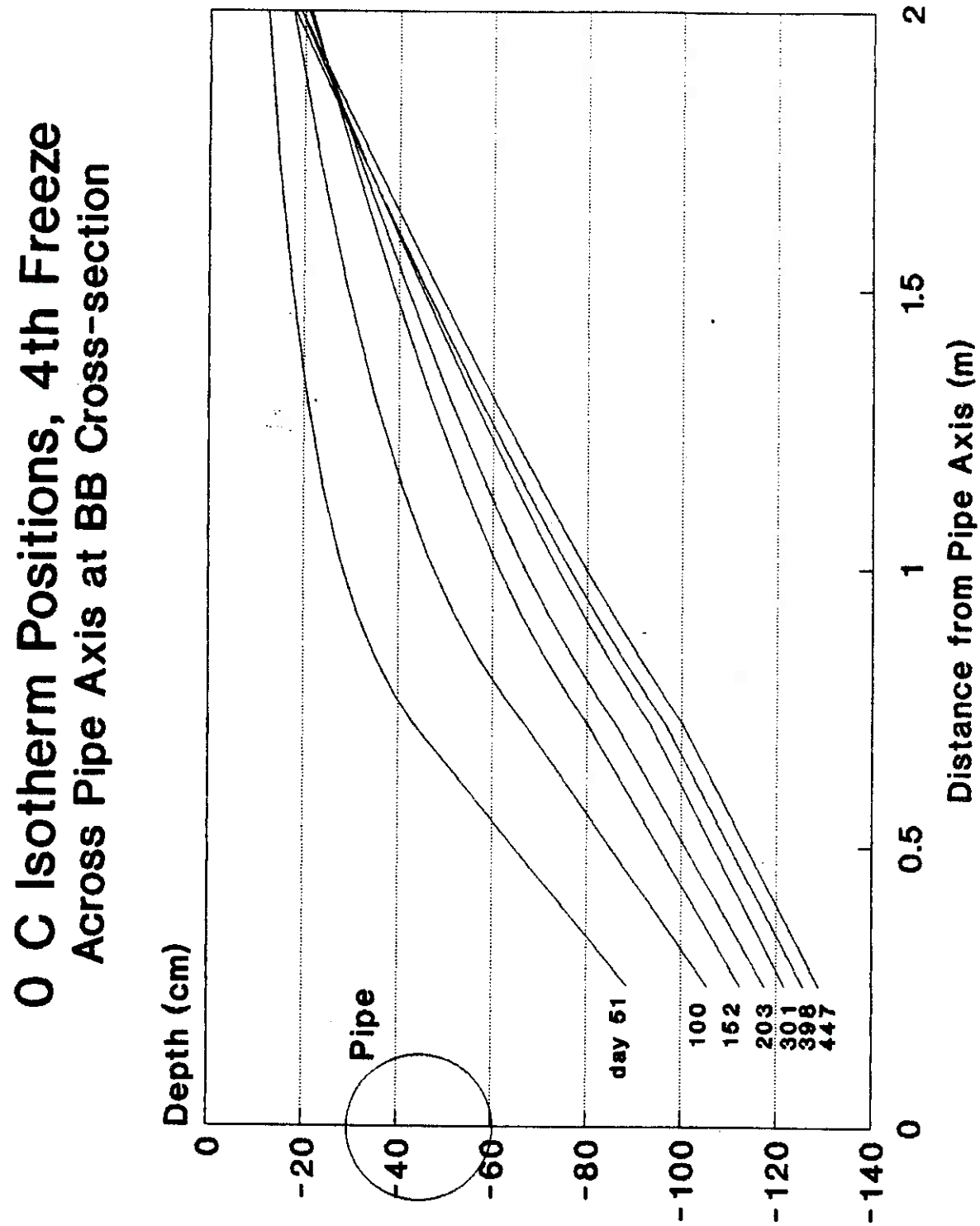
0 C Isotherm Positions, 4th Freeze
Across Pipe Axis at BB Cross-section
Depth (cm)
0
-20
-40
-60
-80
-100
-120
-140
Pipe
day 51
100
152
203
301
398
447
0
0.5
1
1.5
2
Distance from Pipe Axis (m)

Figure 3.4 shows the 0 C isotherm position for the same sites over time. Since the base of the pipe is at about 60 cm, site 2 freezes laterally and vertically quite rapidly. Sites 3 and 4 are decreasingly influenced by the pipe temperatures. One should note that frost penetration at site 5 effectively ceases on about day 150 as does frost heave (see Figure 3.9 and section 3.3).

3.3 Total Heave at Magnet Heave Sites

Table 3.1 shows the total heave obtained on about day 350 during the 3rd and 4th freeze cycle. This date was chosen since it is near the end of the 3rd freeze cycle. Although similar amounts of heave were noted at all sites during both freeze cycles, the patterns of total heave differ.

Table 3.1 Total heave at magnet heave sites, about 350 during the 3rd and 4th freeze

Site	3rd cycle	4th cycle
1	19.3	18.2
2	19.1	17.4
3	17.5	16.7
4	15.1	16.8
5	8.9	4.6
6	17.5	16.5
7	15.5	15.0
8	*	12.6
9	10.7	11.1
10	*	11.1

* unable to determine since bottom magnet could not be reached

3rd cycle day 352
4th cycle day 348

Figure 3.4

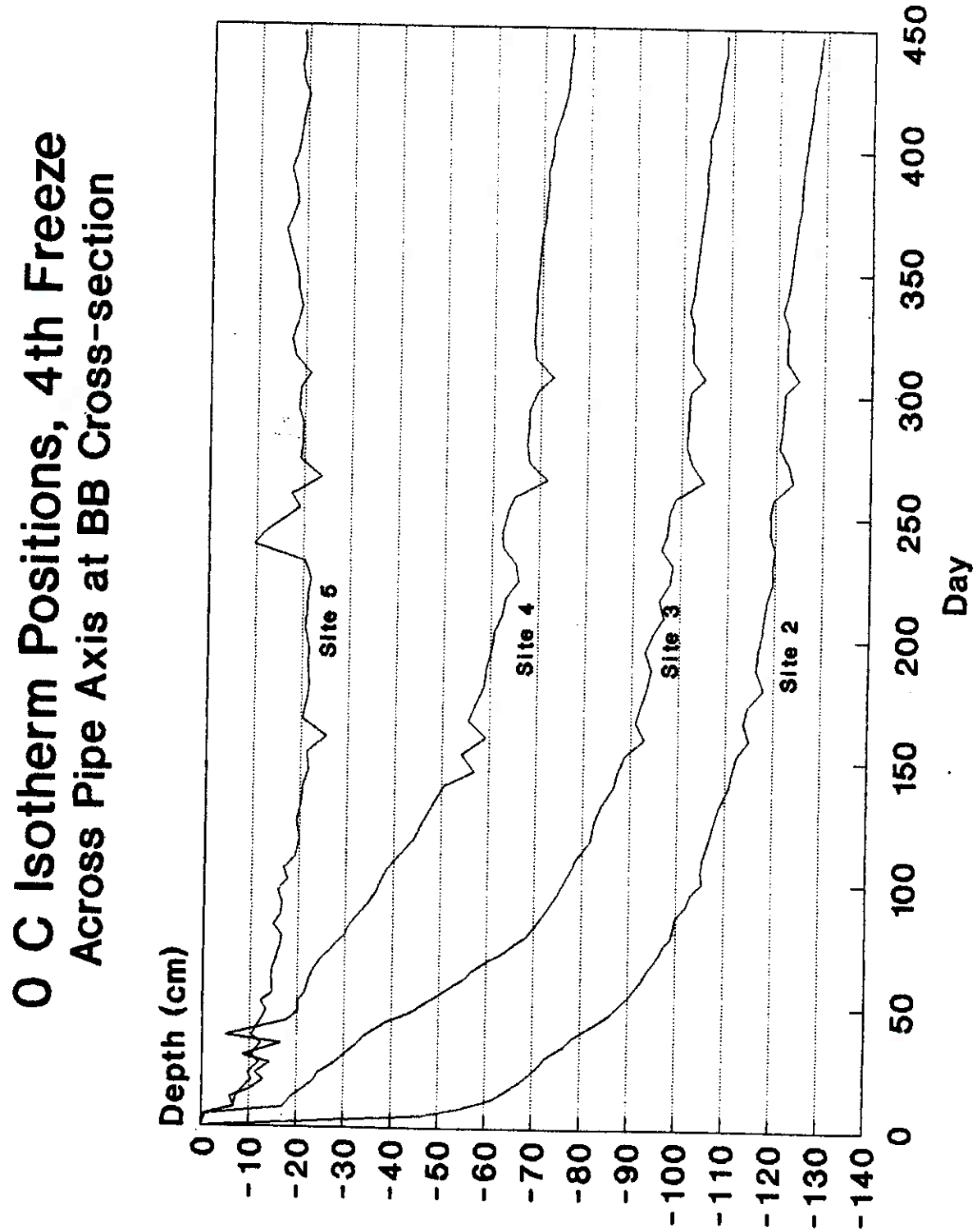
0 C Isotherm Positions, 4th Freeze
Across Pipe Axis at BB Cross-section
Depth (cm)
0
-10
-20
-30
-40
-50
-60
-70
-80
-90
-100
-110
-120
-130
-140
0
50
100
150
200
250
300
350
400
450
Day
Site 5
Site 4
Site 3
Site 2

Figures 3.5 to 3.7 show a comparison of the total heave noted for magnet heave sites 2 to 4 respectively. During the 4th cycle, there was a temporary shutdown of the pipe compressor on about Day 230; this is evident on these figures.

The sites adjacent to the pipe, using magnet site 2 as an example, showed similar amounts of heave up to this point in time (see Figure 3.5) while the sites located away from the pipe axis tended to show greater amounts of heave (see Figures 3.6 and 3.7). Site 5, however, located 2 m from the pipe axis, stopped heaving completely on about Day 150 (as does frost penetration, see Figure 3.4). Frost penetration only reached a depth of about 20 cm during this freeze cycle at this site. In the early stages of the experiment, the greatest temperature gradients were normal to the soil surface. At later dates, the temperature gradients were greatest laterally and it is suspected that water movement was in this direction.

Figures 3.8 and 3.9 show the total heave measured along the pipe axis and across the pipe axis respectively (see Table 2.1 for locations within facility). The pattern shown is essentially the same as that observed during the 3rd cycle with heave decreasing as the sand-silt transition is approached and decreasing as one moves away from the pipe axis. It should be noted that the thermal conditions of sites 1, 2, 6, 7 and 8 are very similar, yet total heave decreases suggesting that the restraining effect of the pipe-frozen annulus is quite

Figure 3.5

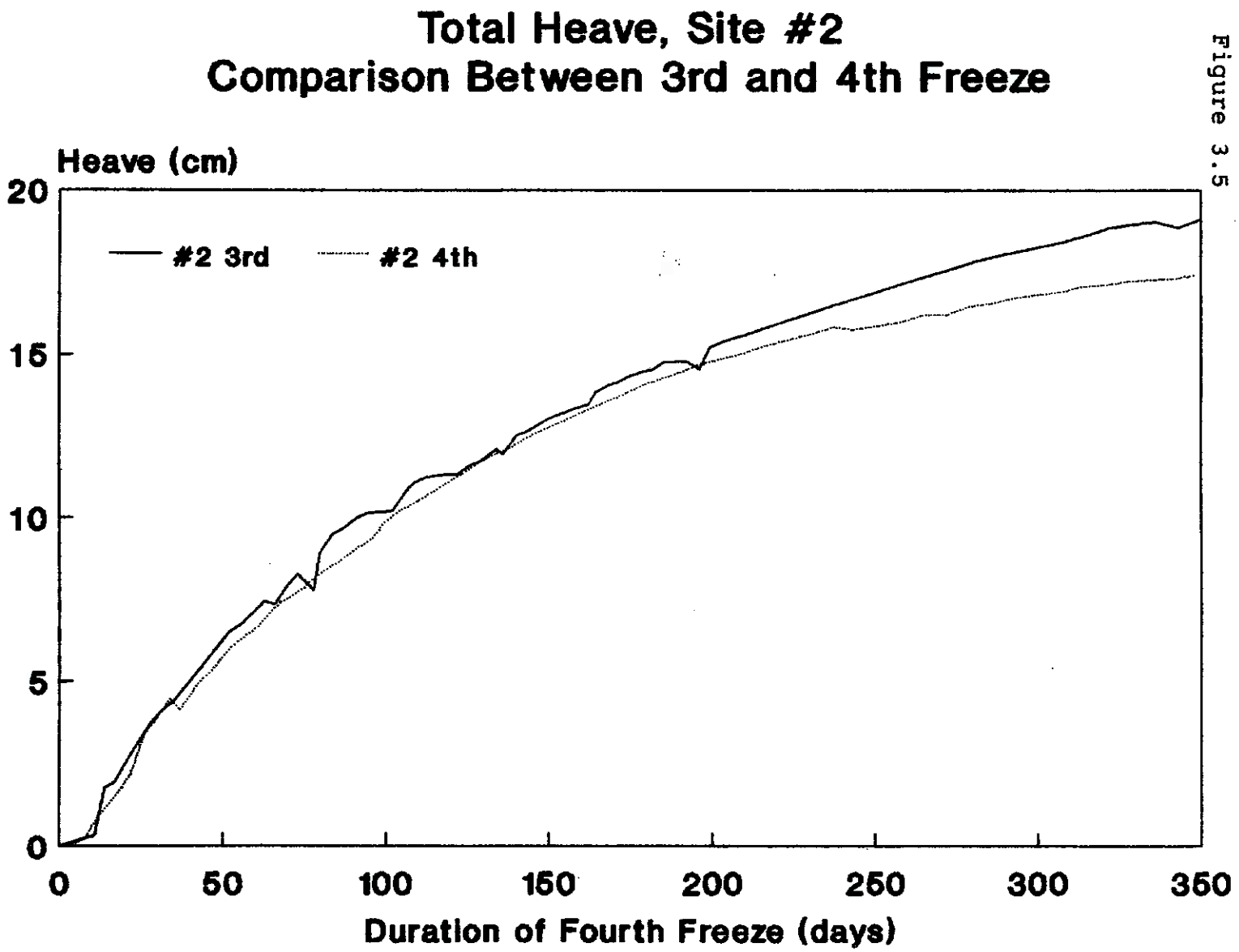
Total Heave, Site #2
Comparison Between 3rd and 4th Freeze
Heave (cm)
#2 3rd
#2 4th
0
5
10
15
20
0
50
100
150
200
250
300
350
Duration of Fourth Freeze (days)

Figure 3.6

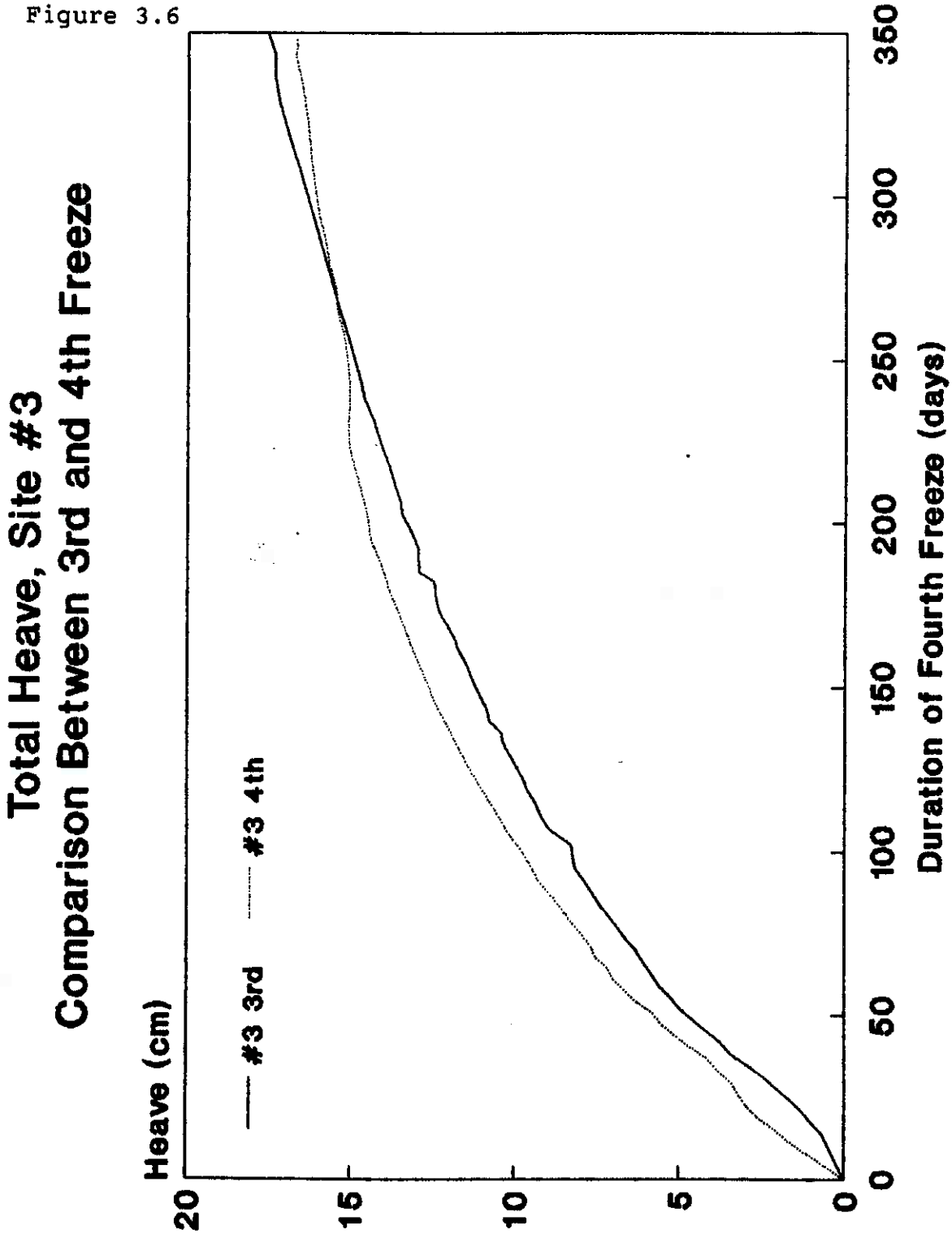
Total Heave, Site #3
Comparison Between 3rd and 4th Freeze
Heave (cm)
#3 3rd
#3 4th
0
5
10
15
20
0
50
100
150
200
250
300
350
Duration of Fourth Freeze (days)

Figure 3.7

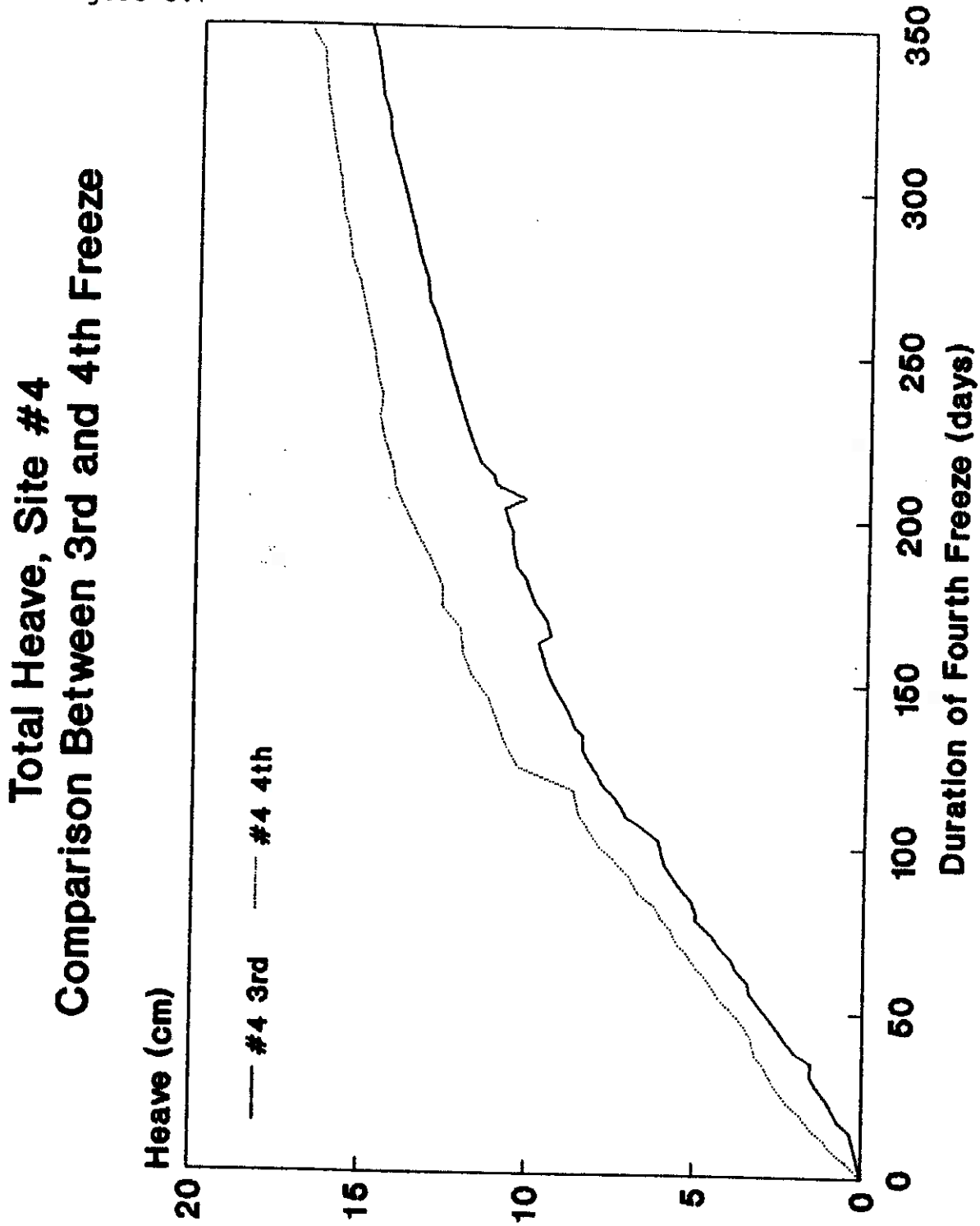
Total Heave, Site #4
Comparison Between 3rd and 4th Freeze
Heave (cm)
#4 3rd
#4 4th
0
5
10
15
20
0
50
100
150
200
250
300
350
Duration of Fourth Freeze (days)

Figure 3.8

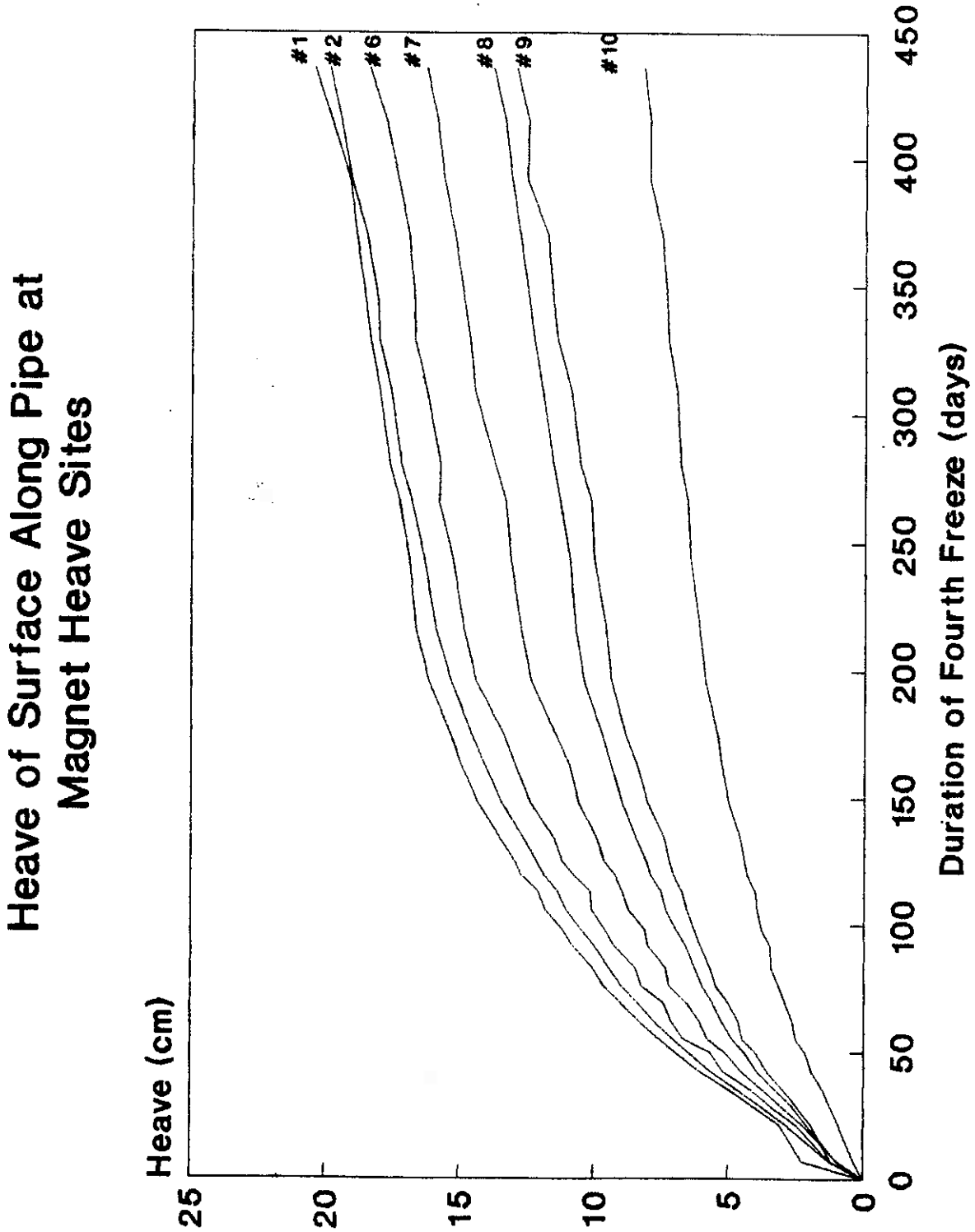
Heave of Surface Along Pipe at
Magnet Heave Sites
Heave (cm)
25
20
15
10
5
0
0
50
100
150
200
250
300
350
400
450
Duration of Fourth Freeze (days)
#1
#2
#6
#7
#8
#9
#10

Figure 3.9

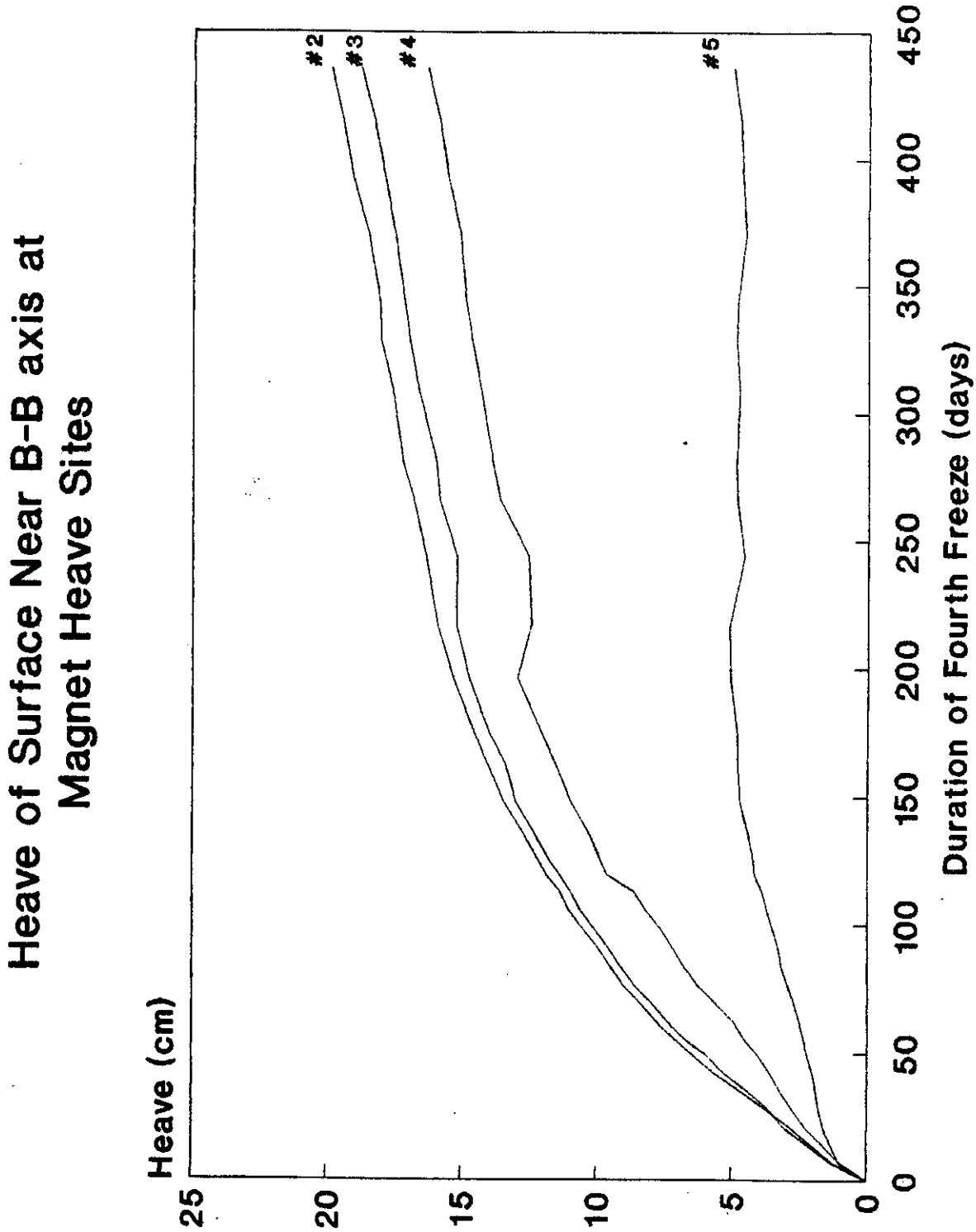
Heave of Surface Near B-B axis at
Magnet Heave Sites
Heave (cm)
25
20
15
10
5
0
0
50
100
150
200
250
300
350
400
450
Duration of Fourth Freeze (days)
#2
#3
#4
#5

significant in controlling total heave.

3.4 Differential Strain at the Magnet Heave Sites

Figures 3.10 to 3.18 show differential strain for magnet heave sites 1 through 10 respectively during the fourth freeze cycle (site 5 has been excluded since the freezing was confined to one soil layer). The depth ranges indicated on these figures denote the initial magnet positions prior to freeze (to the nearest cm). The patterns emerging are similar to those noted during the third freeze cycle. For the sites along the pipe axis, heave tends to decrease the closer the site is to the sand-silt transition (sites 1, 2, 6, 7, 8 and 9). Also, as in the previous cycle, heave decreases the further the site is from the pipe axis (sites 2, 3 and 4).

The strain patterns for all sites show a high initial strain rate with a lower total strain in the early periods of the freeze followed by lower strain rates and greater total strain towards the end of the freeze. These aspects were noted in the previous cycle. As the progression of the freezing front slows, and the temperature gradients become smaller, water movement and ice accumulation will be greater per unit volume.

It should also be noted that the amount of strain in already frozen ground is quite significant at some depths towards the latter part of the freeze cycle, particularly for the sites located off-axis (see Figures 3.12 and 3.13). At site 3 (located 65 cm off the pipe axis), the 59-72 cm layer has experienced

Figure 3.10

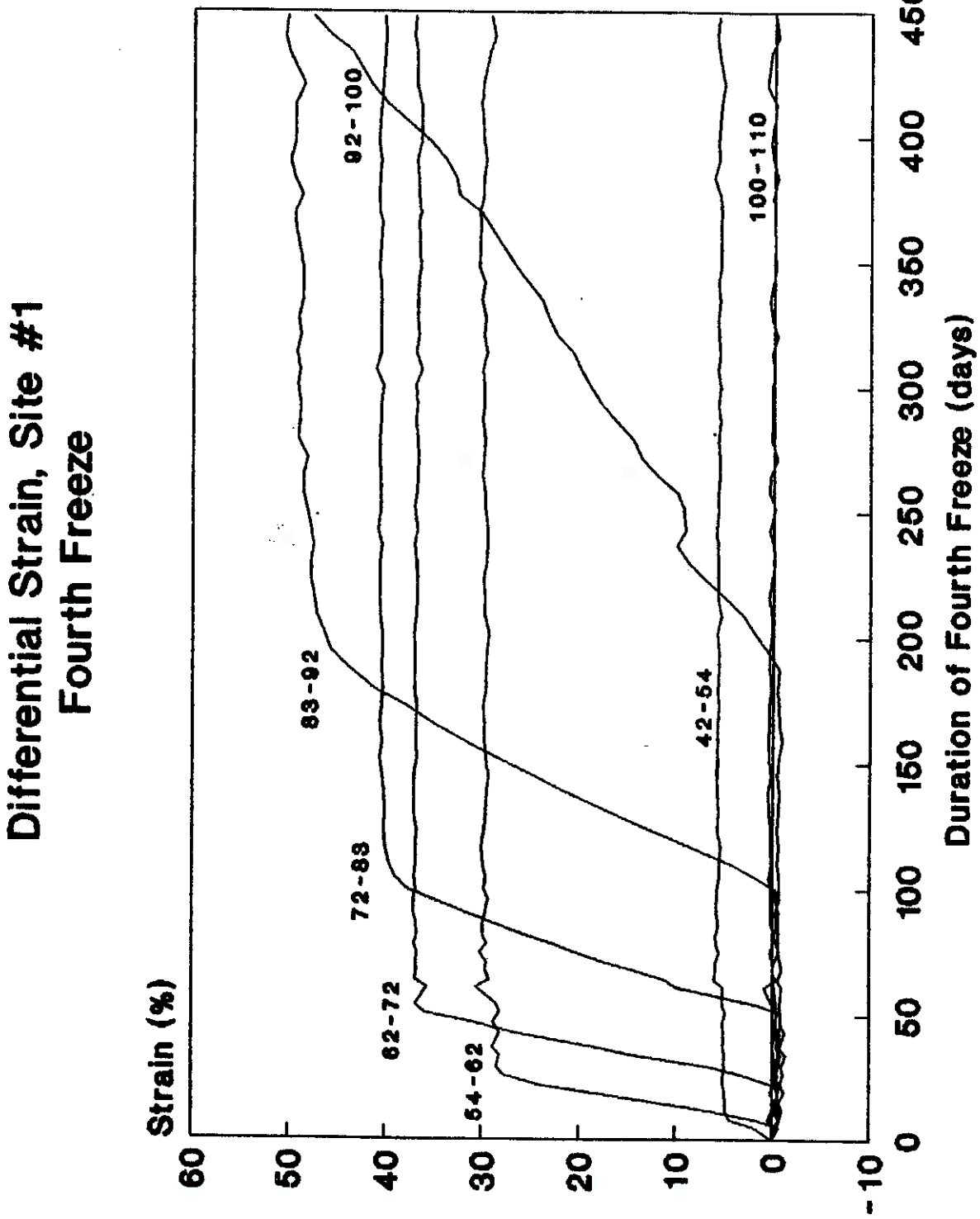
Differential Strain, Site #1
Fourth Freeze
Strain (%)
60
50
40
30
20
10
0
-10
0
50
100
150
200
250
300
350
400
450
Duration of Fourth Freeze (days)
92-100
83-92
72-83
62-72
54-62
42-54
100-110

Figure 3.11

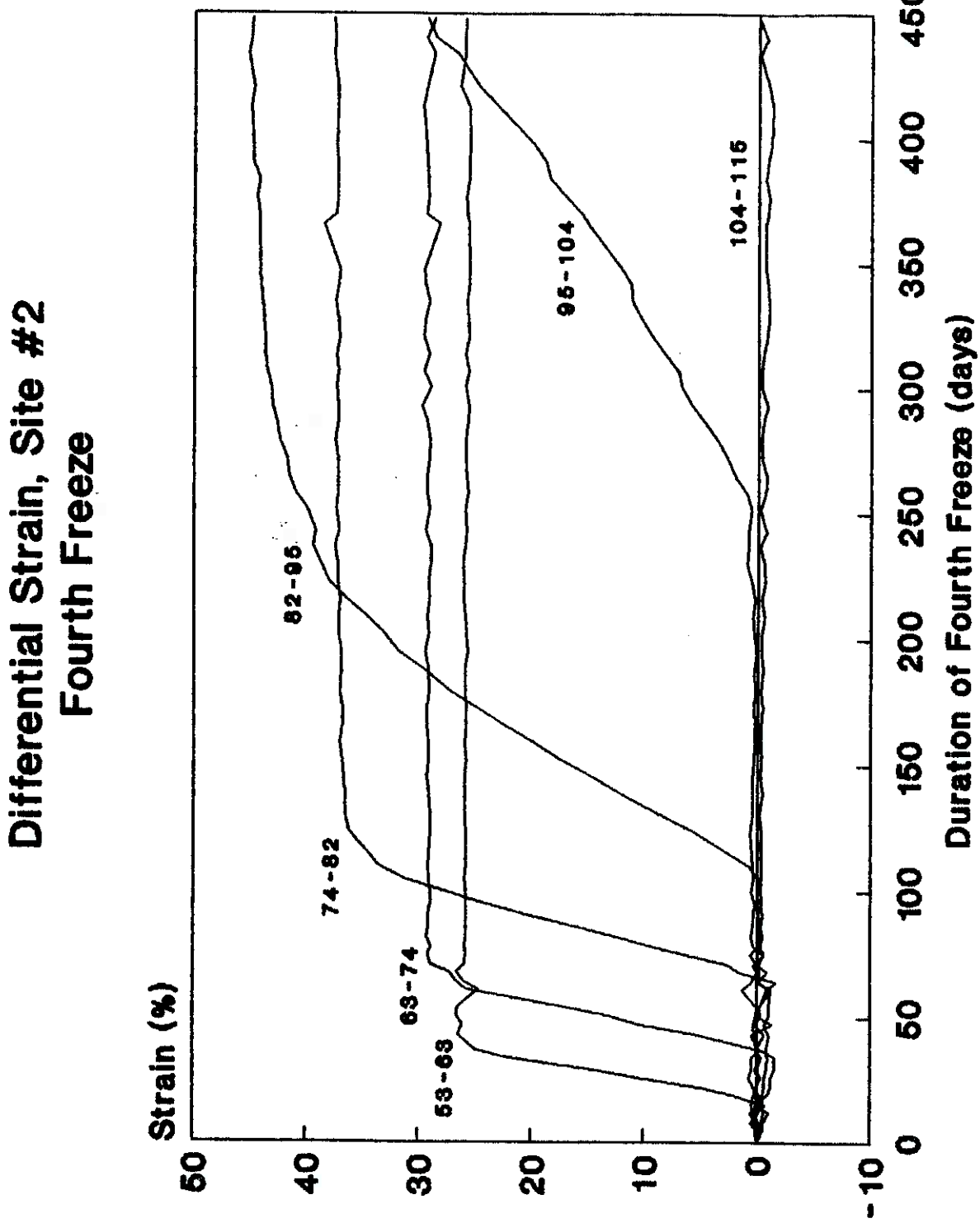
Differential Strain, Site #2
Fourth Freeze
Strain (%)
50
40
30
20
10
0
-10
0
50
100
150
200
250
300
350
400
450
Duration of Fourth Freeze (days)
82-95
74-82
63-74
53-63
95-104
104-115

Figure 3.12

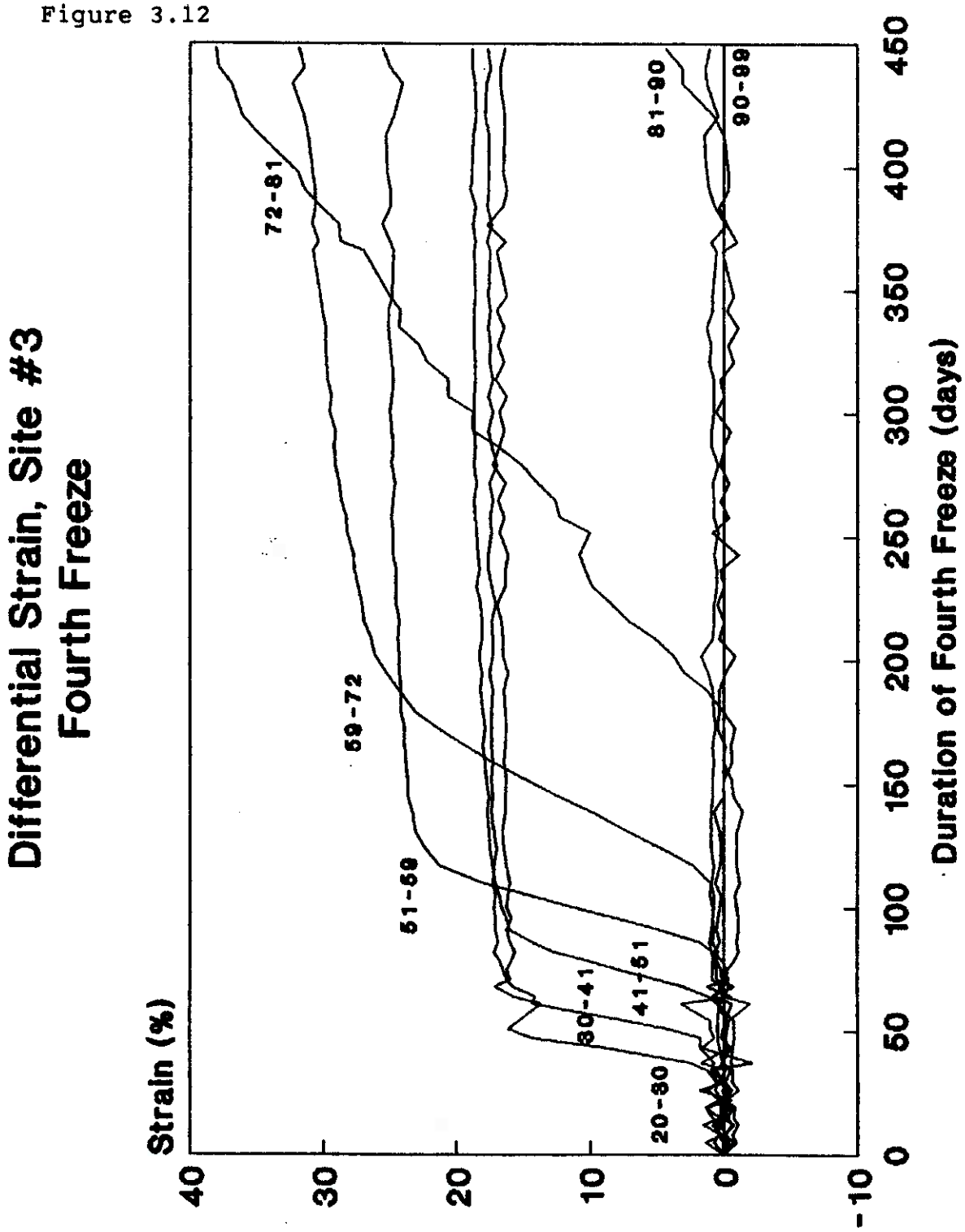
Differential Strain, Site #3
Fourth Freeze
Strain (%)
40
30
20
10
0
-10
0
50
100
150
200
250
300
350
400
450
Duration of Fourth Freeze (days)
72-81
59-72
51-59
30-41
41-51
20-30
81-90
90-99

Figure 3.13

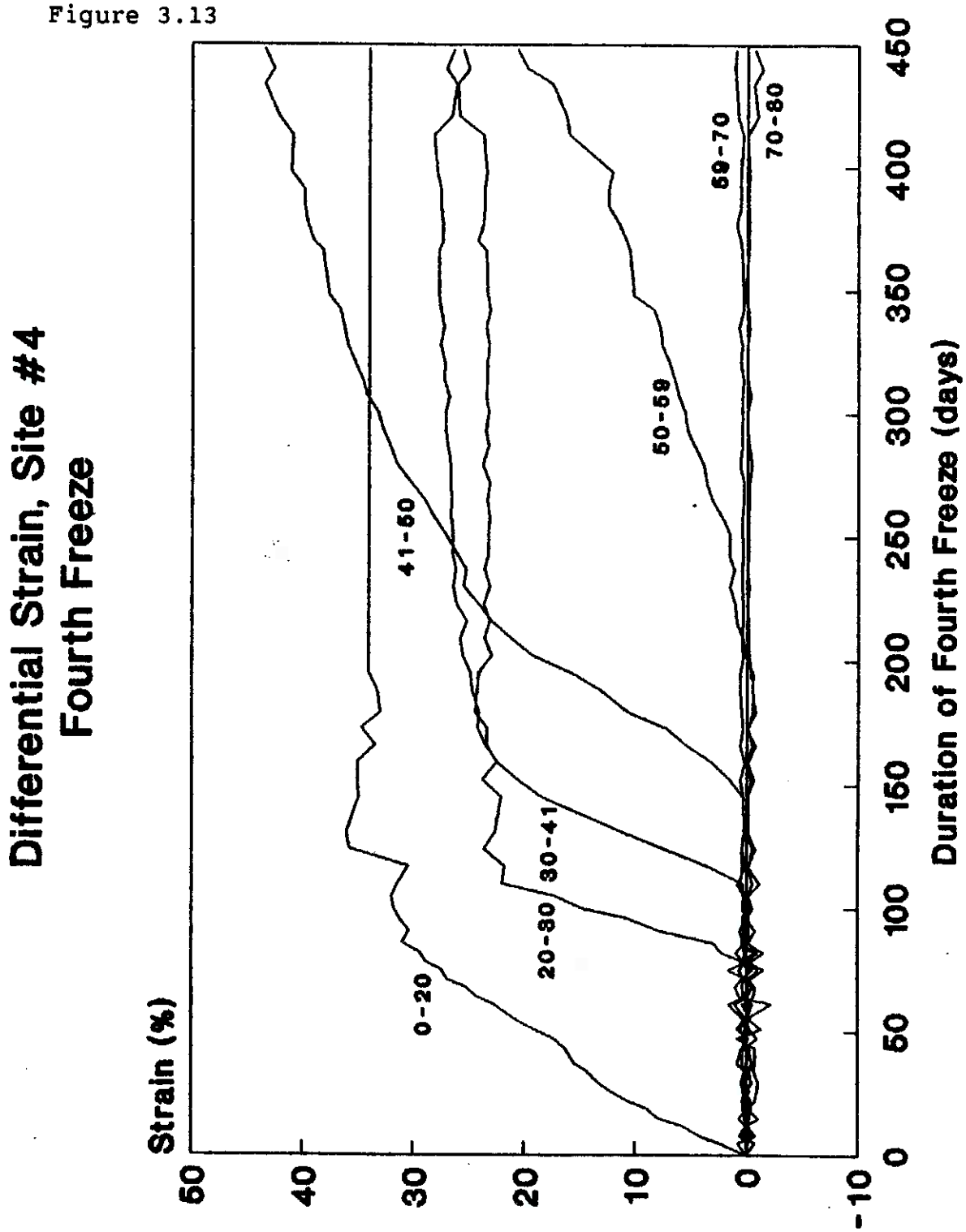
Differential Strain, Site #4
Fourth Freeze
Strain (%)
Duration of Fourth Freeze (days)
0-20
20-30
30-41
41-50
50-59
59-70
70-80
60
40
30
20
10
0
-10
0
50
100
150
200
250
300
350
400
450

Figure 3.14

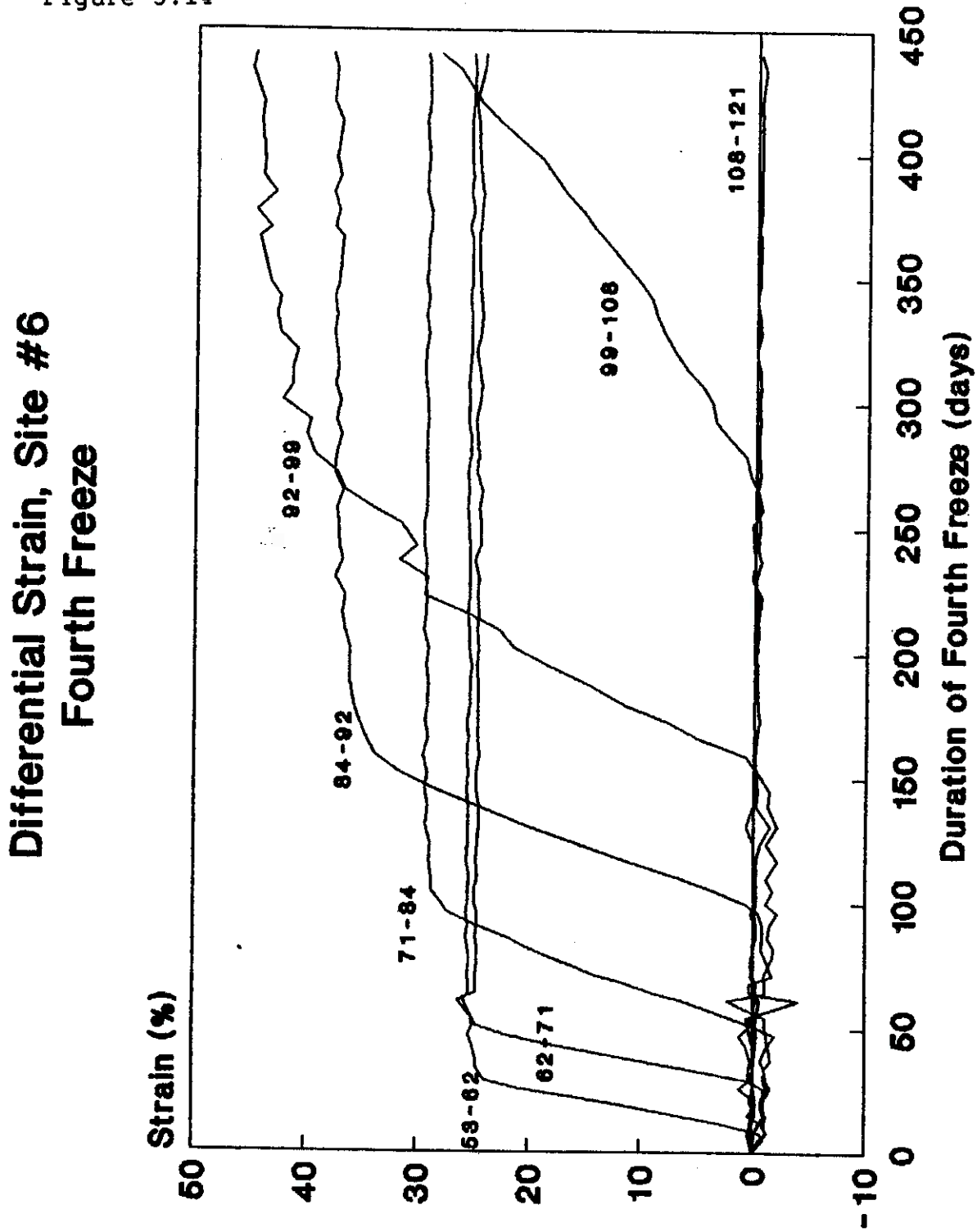
Differential Strain, Site #6
Fourth Freeze
Strain (%)
50
40
30
20
10
0
-10
0
50
100
150
200
250
300
350
400
450
Duration of Fourth Freeze (days)
92-99
84-92
71-84
62-71
53-62
99-108
108-121

Figure 3.15

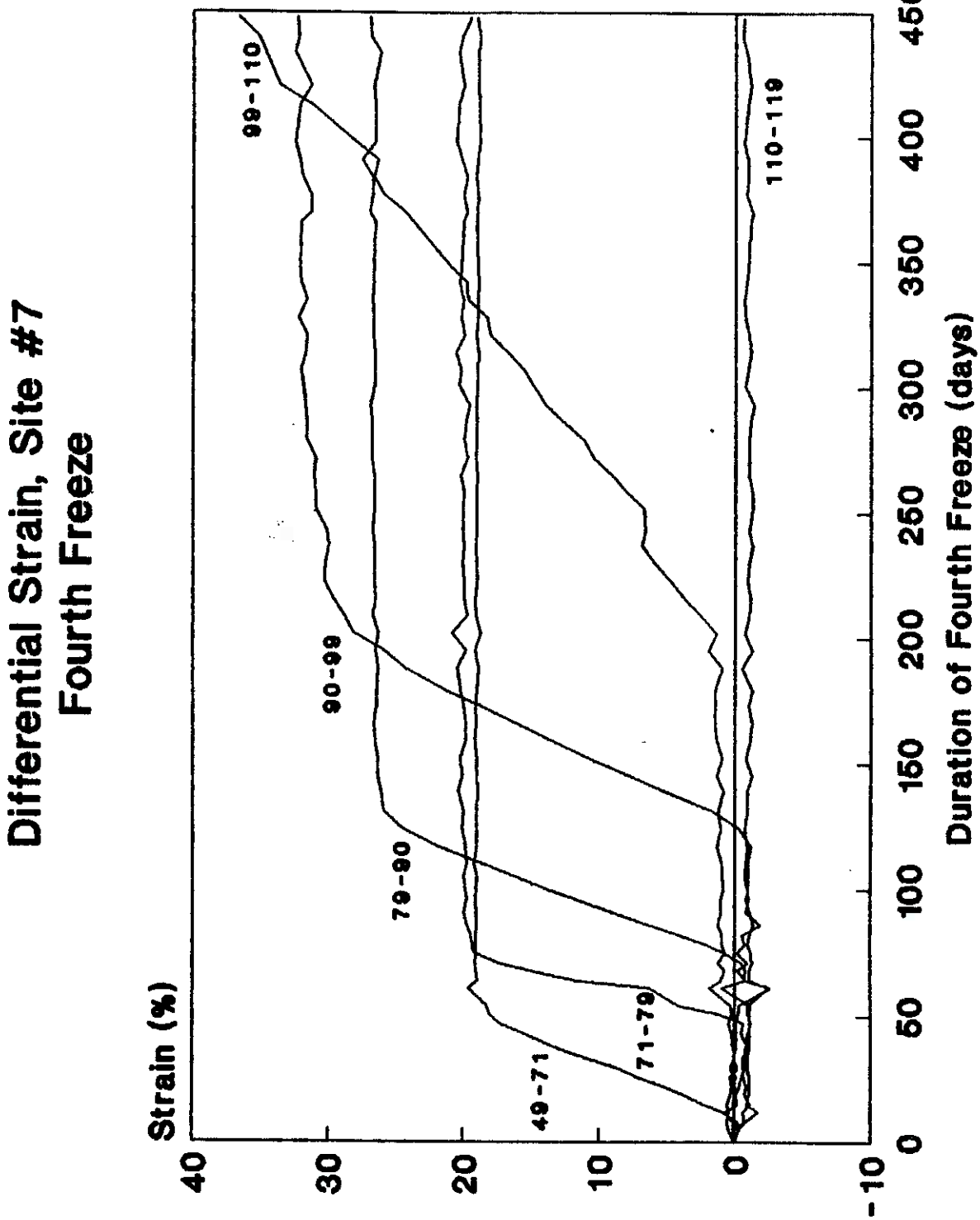
Differential Strain, Site #7
Fourth Freeze
Strain (%)
40
30
20
10
0
-10
0
50
100
150
200
250
300
350
400
450
Duration of Fourth Freeze (days)
99-110
90-99
79-90
71-79
49-71
110-119

Figure 3.16

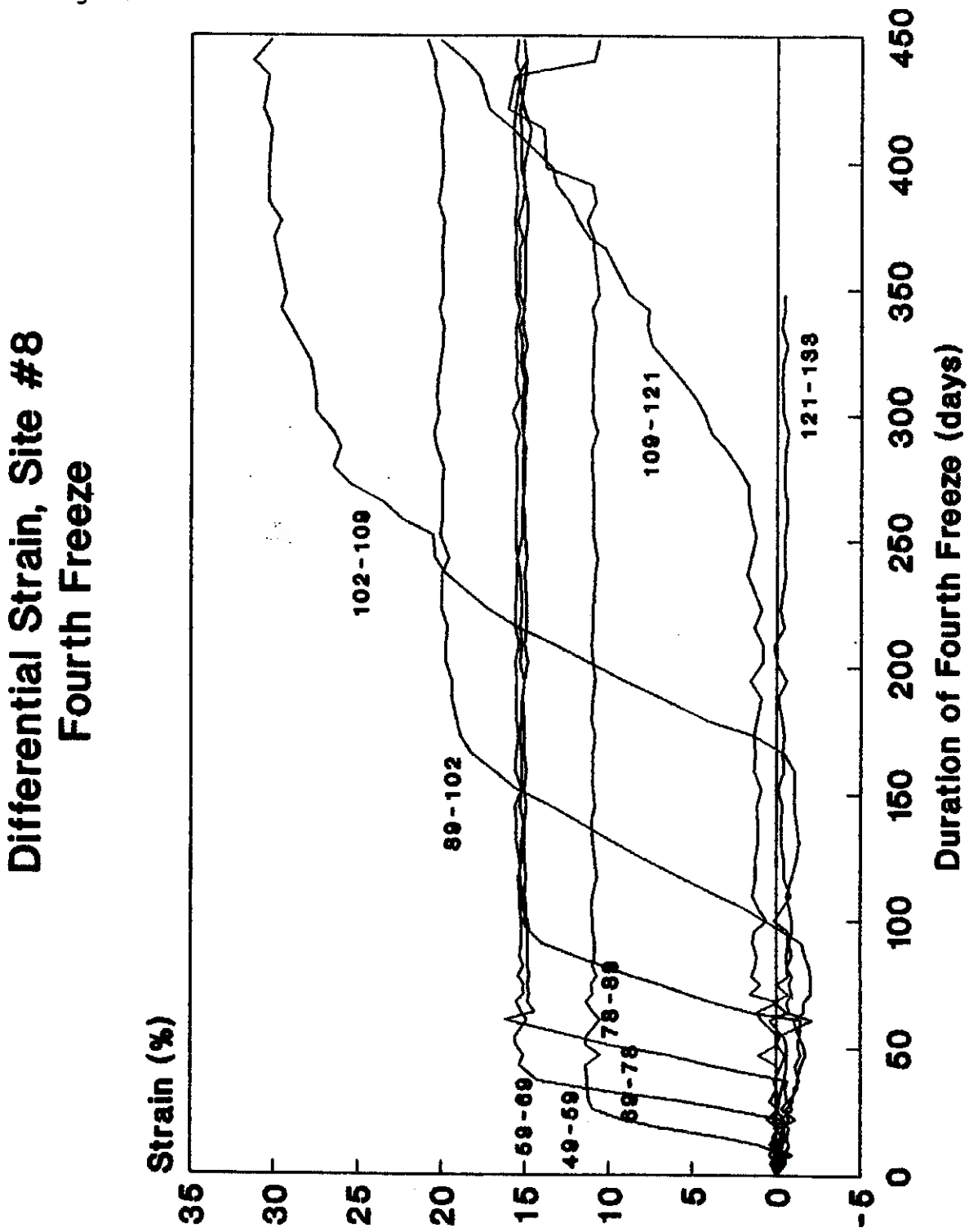
Differential Strain, Site #8
Fourth Freeze
Strain (%)
35
30
25
20
15
10
5
0
-5
0
50
100
150
200
250
300
350
400
450
Duration of Fourth Freeze (days)
102-109
89-102
109-121
121-138
59-69
49-59
69-78
78-89

Figure 3.17

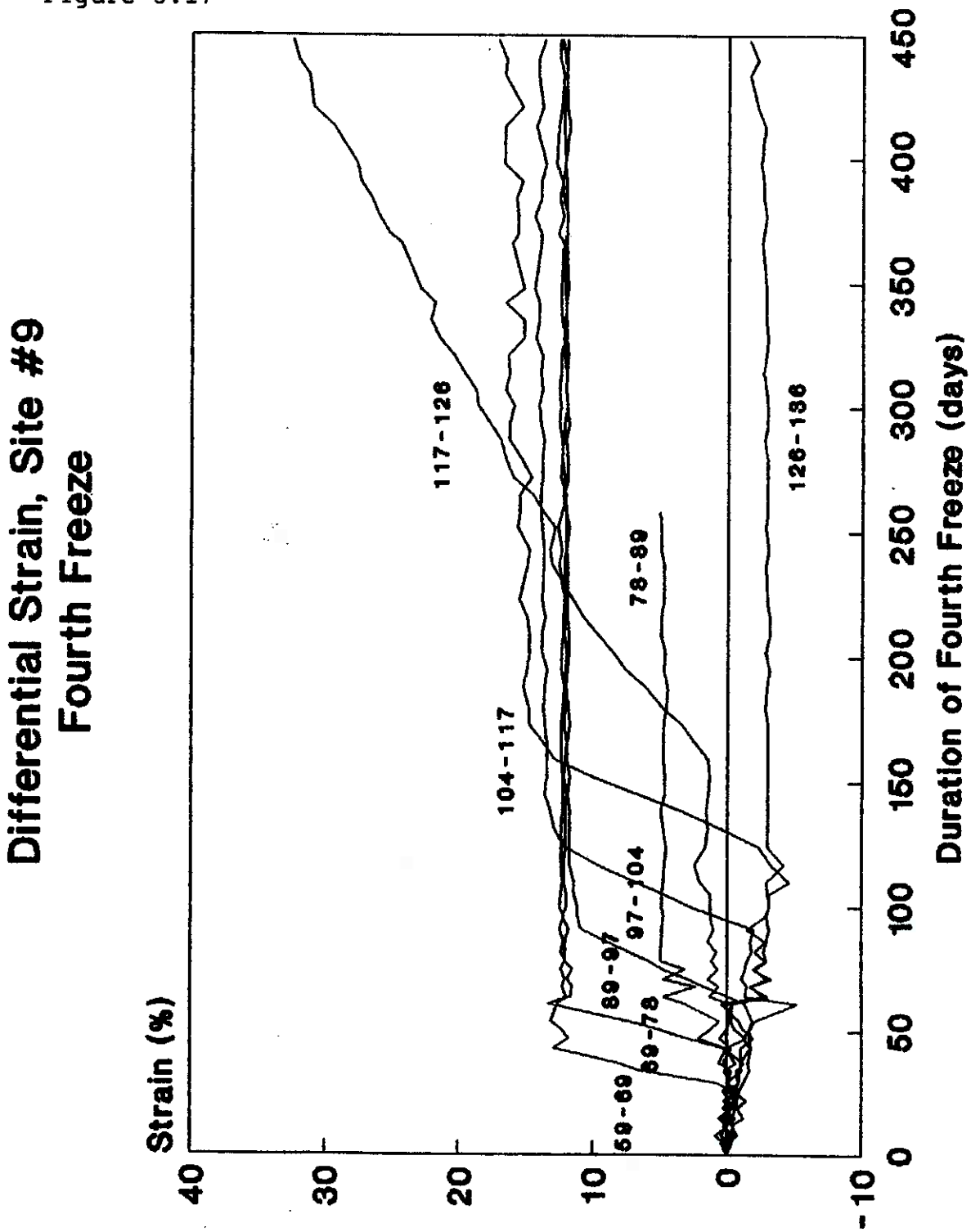
Differential Strain, Site #9
Fourth Freeze
Strain (%)
40
30
20
10
0
-10
0
50
100
150
200
250
300
350
400
450
Duration of Fourth Freeze (days)
117-126
104-117
78-89
126-136
97-104
89-97
59-69
69-78

Figure 3.18

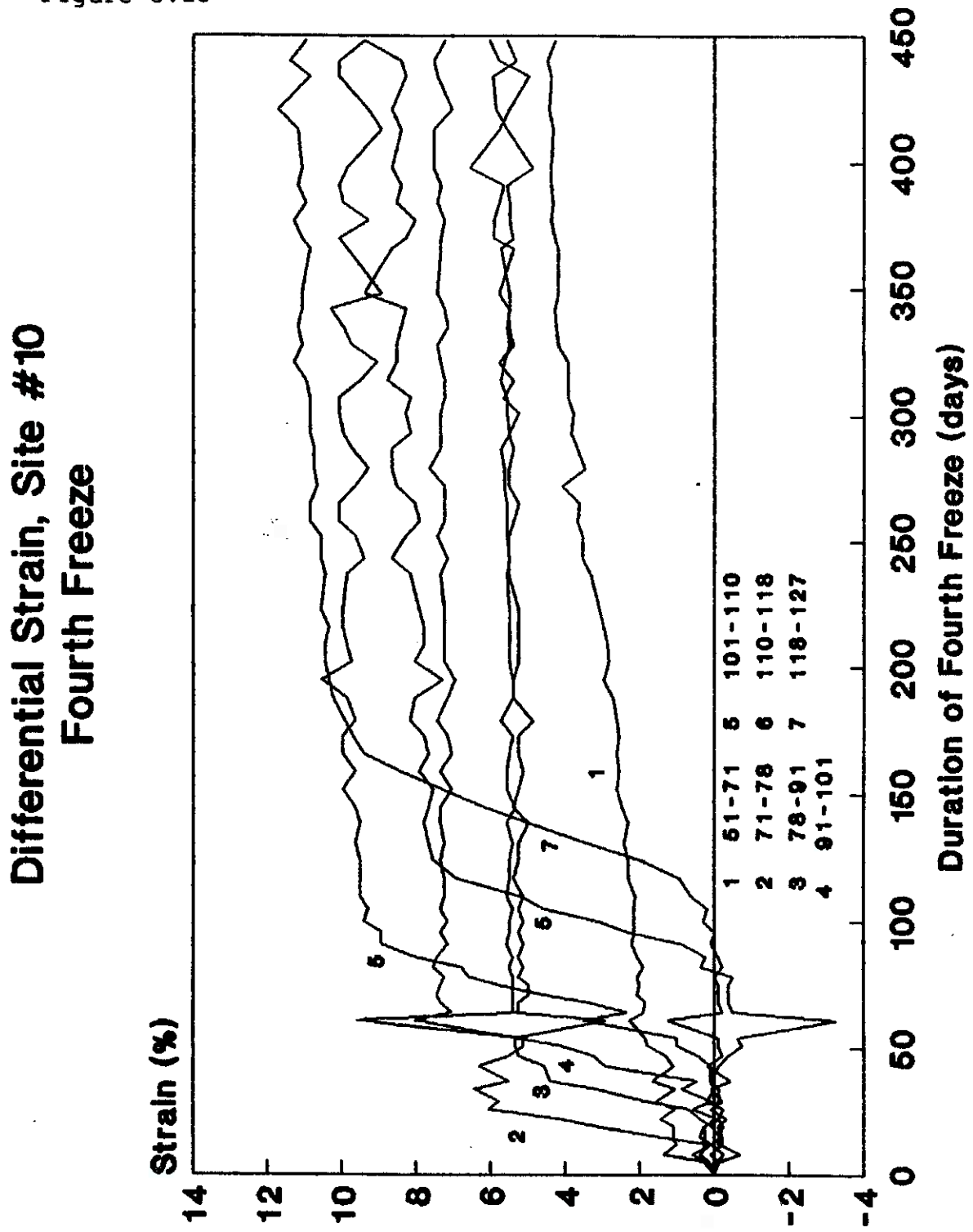
Differential Strain, Site #10
Fourth Freeze
Strain (%)
14
12
10
8
6
4
2
0
-2
-4
0
50
100
150
200
250
300
350
400
450
Duration of Fourth Freeze (days)
1 51-71
2 71-78
3 78-91
4 91-101
5 101-110
6 110-118
7 118-127

about 24% strain when the 72-81 cm layer begins to heave; ultimately the 59-72 cm layer exhibited a strain of about 32% at Day 450 with 8% occurring in already frozen ground (see Figure 3.12).

Site 4 (located 1.0 m off the pipe axis) shows an even greater amount of strain within already frozen ground as evidenced by the 41-50 cm layer. This layer experienced about 25% strain by day 250 when the 50-59 cm layer began to strain. by day 450, the 41-50 cm layer had undergone about 43% strain, the difference (18%) having occurred in already frozen ground (see Figure 3.13).

The strain pattern at magnet site 9 has been complicated by a quite severe deformation of the access tube (for lowering the magnet sensor) and an apparent breakage of one or more of the magnet rings (see Figure 3.17). The deformation made it progressively difficult to lower the magnet sensor and the curvature of the access tube may be binding certain magnet rings. The apparent breakage has resulted in "ghost" magnets appearing, often separated by a centimetre or two suggesting one of the three ring magnets has come loose from the plexiglass support disk or the disk has broken into several pieces. Excavation at the end of the 4th thaw will solve this mystery.

The strain pattern for magnet site 10, located in the sand section near the transition, suggests that the pipe-frozen ground annulus may be pulling the soil apart as the pipe is uplifted. This seems to be the case for layer 1 (51-71 cm) which appears to

be continuing to strain after it is frozen in (see Figure 3.18). Since the soil is sandy, and the other layers don't exhibit this phenomenon, the apparent expansion in this layer is probably attributable to lateral cracking and uplift.

3.5 Pipe displacement

Figure 3.19 shows the pipe shape at the start of the four freeze cycles. It is apparent that the pipe has been unable to return to its original position (freeze cycle 1) after a freeze thaw cycle. The pipe is increasingly being displaced upward within the silt section as has been reported previously. The gap beneath the pipe in the silt section has probably developed because of the difference in settlement patterns between the soil and the pipe.

Figure 3.20 shows the pipe position for selected dates during the fourth freeze cycle while Figure 3.21 shows the heave measured since the start of the cycle. The pattern is in keeping with that observed in previous freeze cycles. The total heave could have been more if it were not for the compressor shut-down on Day 230.

3.6 Pipe stress

Pipe stress observations on about day 350 for the 2nd, 3rd and 4th freeze cycles is shown in Figure 3.22. The evolution of pipe stress for selected dates during the 4th freeze cycle is shown in Figure 3.23. Note that some gauges in the silt section

Figure 3.19

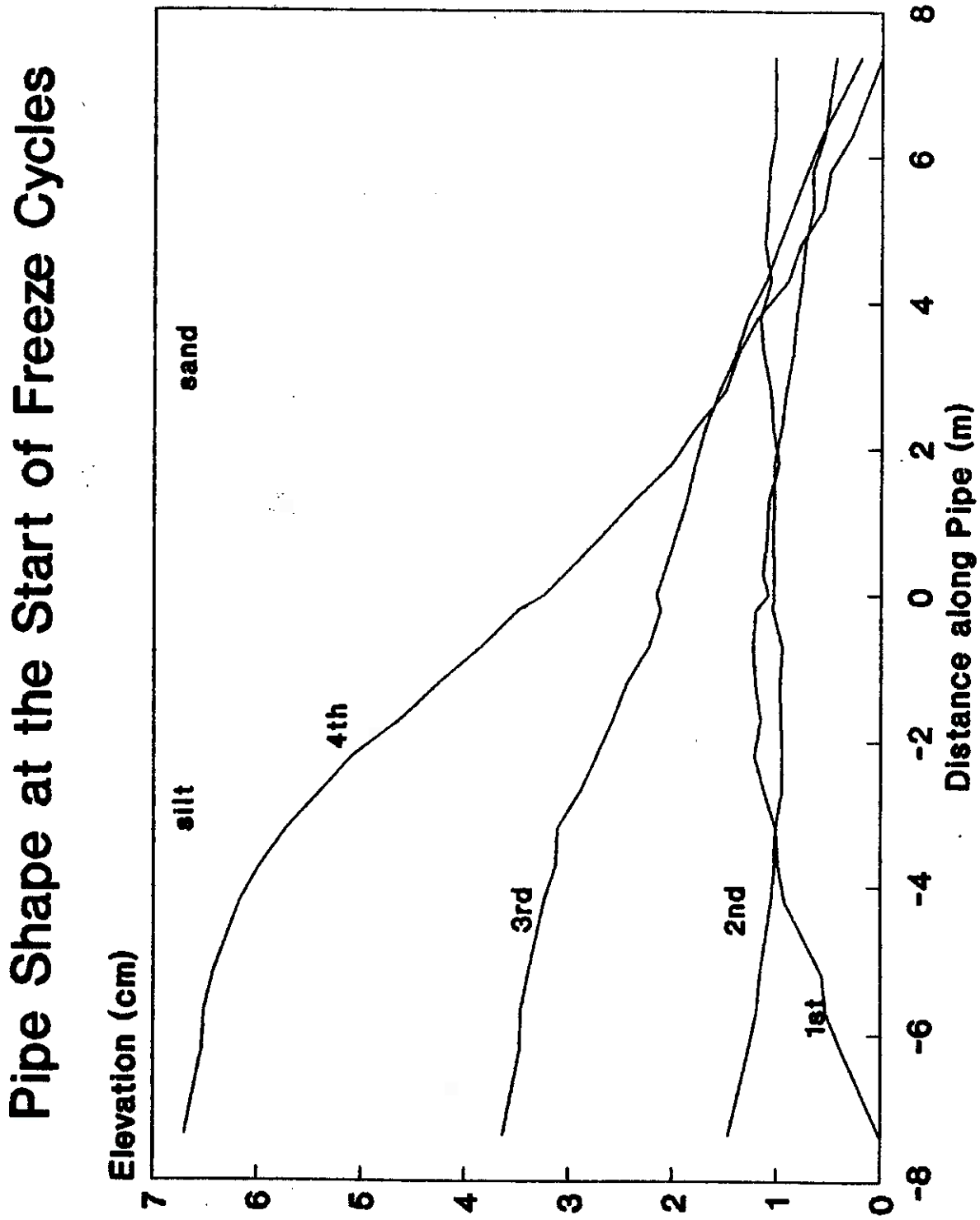
Pipe Shape at the Start of Freeze Cycles
Elevation (cm)
7
6
5
4
3
2
1
0
silt
sand
4th
3rd
2nd
1st
-8
-6
-4
-2
0
2
4
6
8
Distance along Pipe (m)

Figure 3.20

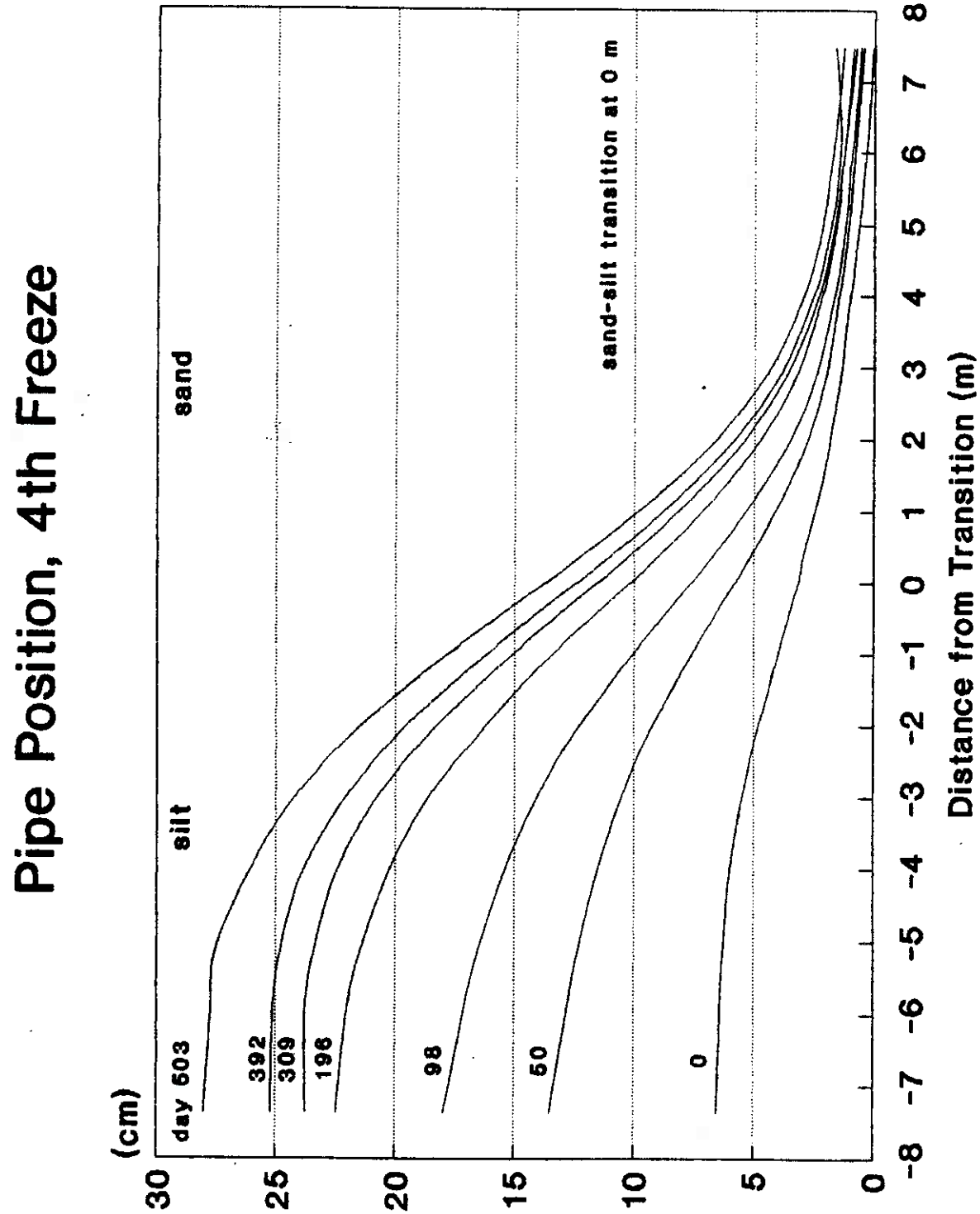
Pipe Position, 4th Freeze
(cm)
silt
sand
day 503
392
309
196
98
50
0
sand-silt transition at 0 m
30
25
20
15
10
5
0
-8
-7
-6
-5
-4
-3
-2
-1
0
1
2
3
4
5
6
7
8
Distance from Transition (m)

Figure 3.21

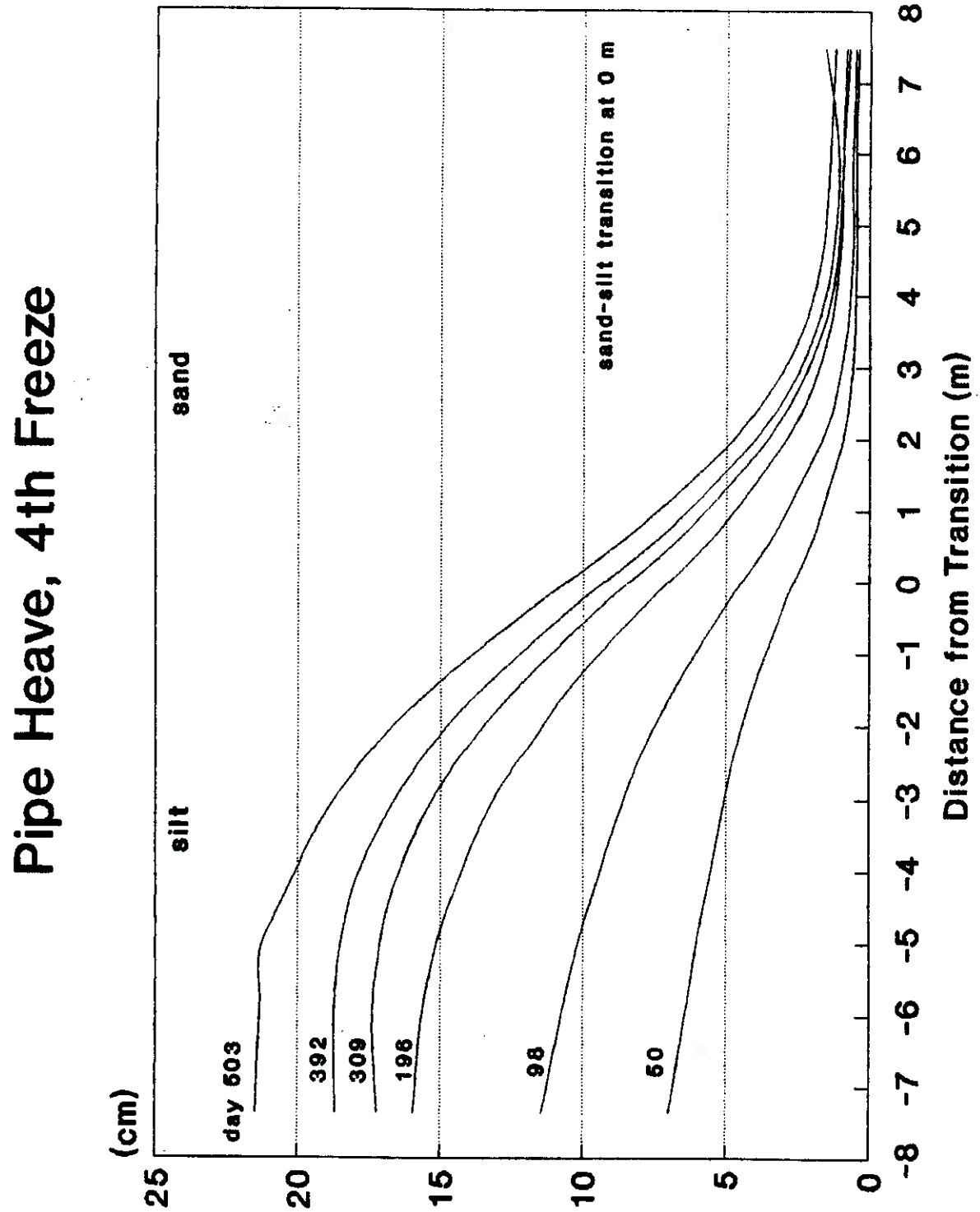
Pipe Heave, 4th Freeze
(cm)
silt
sand
sand-silt transition at 0 m
day 503
392
309
196
98
50
25
20
15
10
5
0
-8
-7
-6
-5
-4
-3
-2
-1
0
1
2
3
4
5
6
7
8
Distance from Transition (m)

Figure 3.22

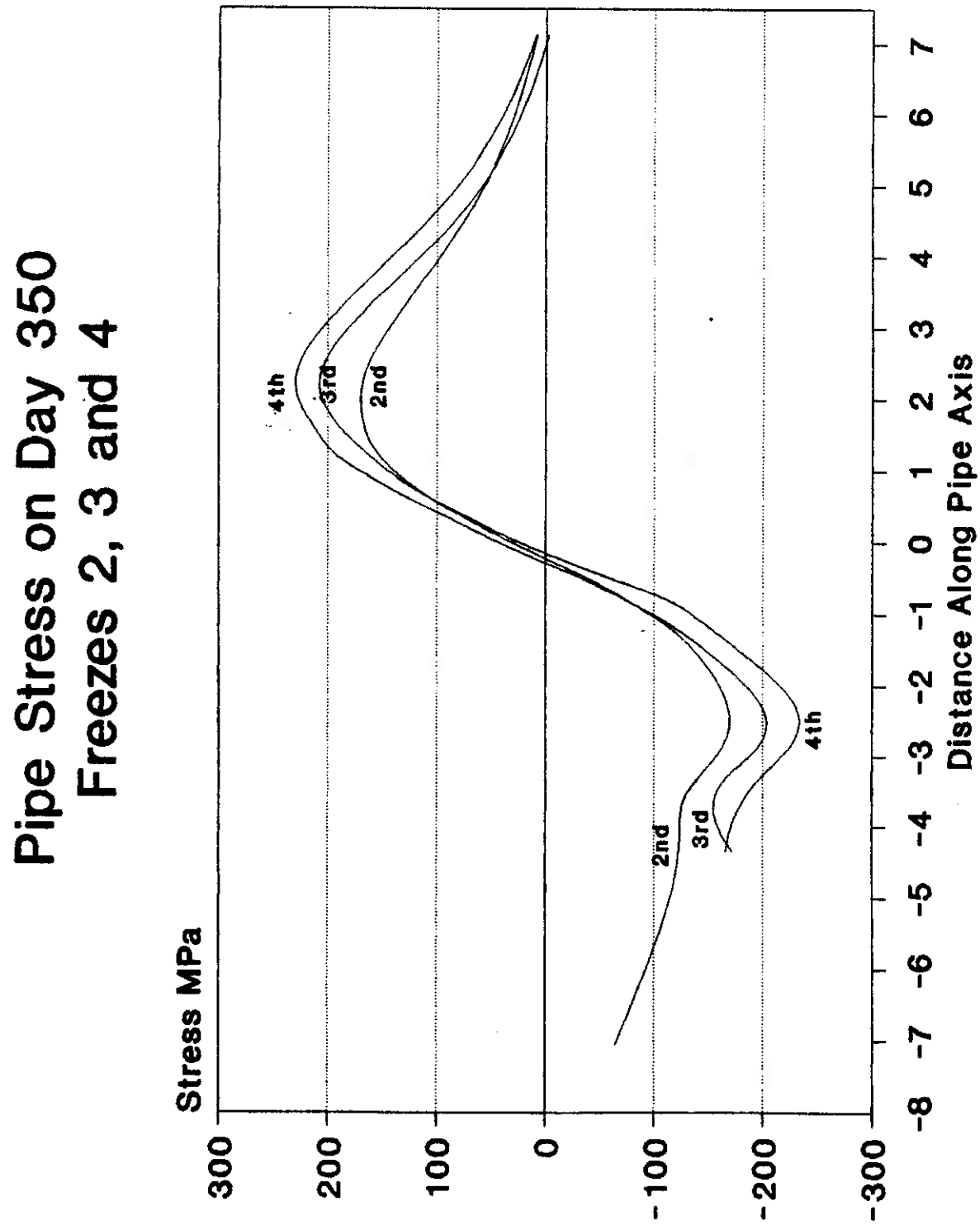
Pipe Stress on Day 350
Freezes 2, 3 and 4
Stress MPa
300
200
100
0
-100
-200
-300
-8
-7
-6
-5
-4
-3
-2
-1
0
1
2
3
4
5
6
7
Distance Along Pipe Axis
4th
3rd
2nd
2nd
3rd
4th

Figure 3.23

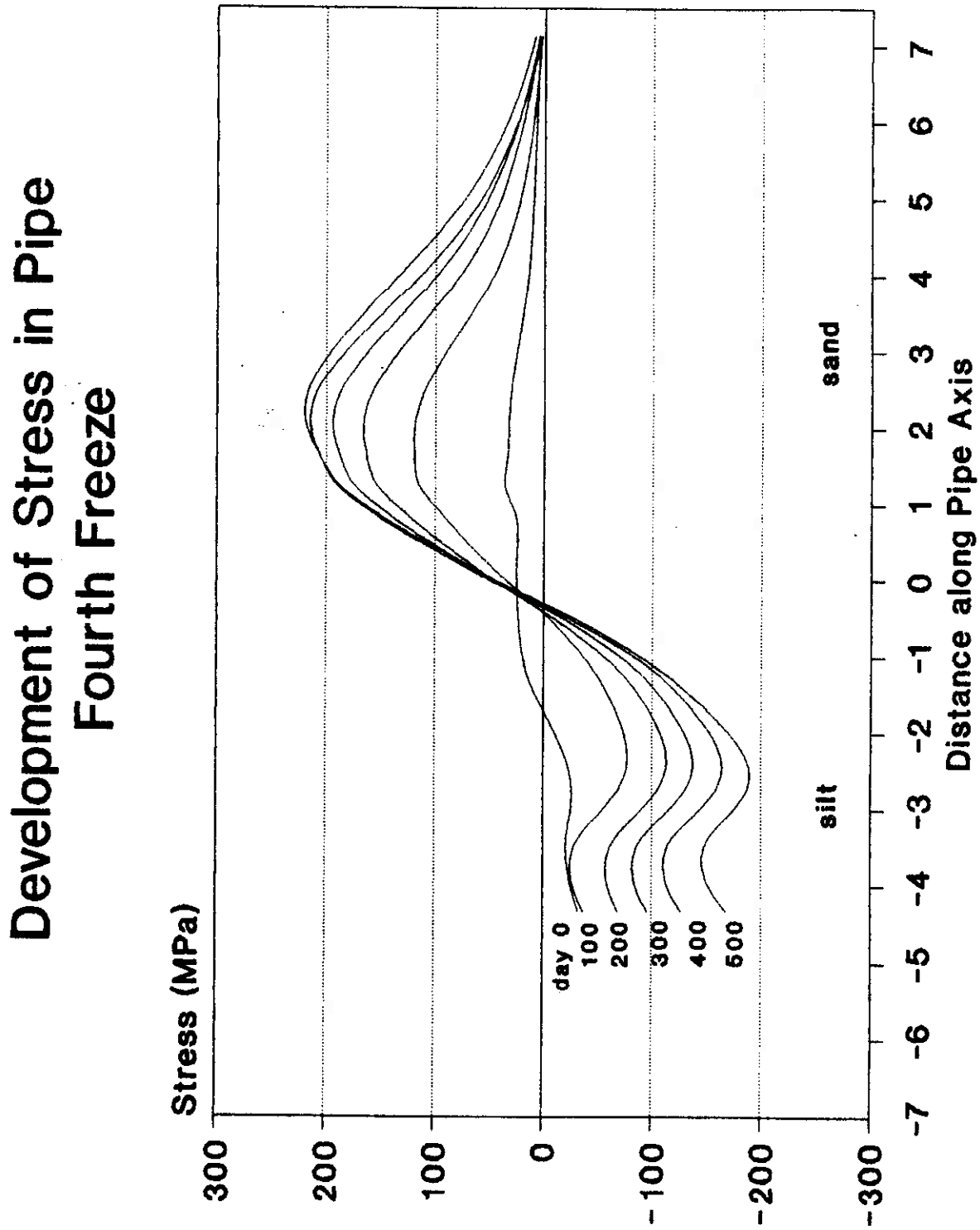
Development of Stress in Pipe
Fourth Freeze
Stress (MPa)
300
200
100
0
-100
-200
-300
day 0
100
200
300
400
500
silt
sand
-7
-6
-5
-4
-3
-2
-1
0
1
2
3
4
5
6
7
Distance along Pipe Axis

broke during the 3rd freeze and will be replaced when the facility is refurbished.

Stress levels have been increasing between cycles, this may in part be due to the residual stresses resulting from differences in the initial position of the pipe prior to freeze (see section 3.5).

3.7 Soil Pressures

3.7.1 Petur Cells

The Petur cells were excavated and refurbished prior to the fourth freeze cycle. Many of the cells failed during the third freeze cycle because the oil-filled rubber bulbs which cover the diaphragm leaked. The initial failure seems to have occurred because the rubber was not very strong and seemed to weaken when in contact with soil water for extended periods of time. A new type of rubber bulb was used which did not weaken when wet and was more robust.

Soil pressures beneath the pipe near the B-B transition in the silt section are shown in Figure 3.24. Pressure values are given in millibars (10 mb = 1 KPa) and are shown as the <u>change</u> since Day 0 of the 4th freeze to remove the effects of overburden pressures and residual pressures which arise during sensor assembly.

The sensor depths refer to their initial placement beneath the soil surface prior to the fourth freeze (the 80 cm sensor is approximately 27 cm beneath the pipe). The pressure values for

Figure 3.24

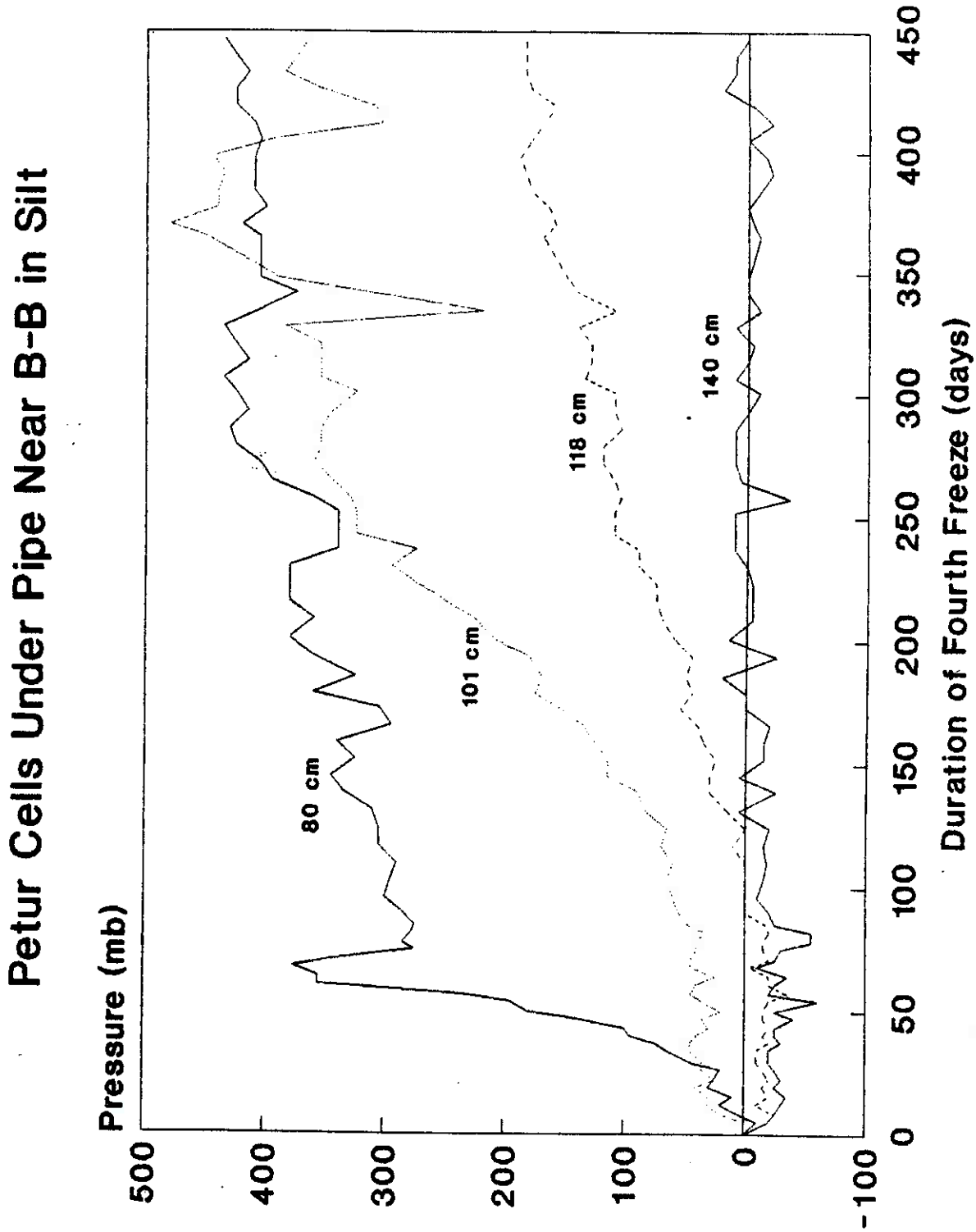
Petur Cells Under Pipe Near B-B in Silt
Pressure (mb)
500
400
300
200
100
0
-100
0
50
100
150
200
250
300
350
400
450
Duration of Fourth Freeze (days)
80 cm
101 cm
118 cm
140 cm

the Petur cells at this location increased some days before the 0 C isotherm reached their position. This observation can be attributed to a reaction stress within the unfrozen ground. Ground consolidation was not noted in the differential strain observations near B-B (see Figure 3.11).

The 80 cm sensor recorded a marked increase in pressure after the first 25 days of the freeze. By day 60, the sensor was well within frozen ground and continuing increases in pressure were noted after this date. Pressure values for the 101 cm sensor remained fairly constant until about day 80. Between day 80 and 270 the recorded pressure changed from about 40 mb to 360 mb, after day 270 pressure levels continued to increase but in a much more erratic fashion than the 80 cm sensor. The soil pressures recorded by the 118 cm sensor also began to increase slightly on about day 90 and continued to rise until the end of the freeze cycle. This cell remained within unfrozen ground during the course of the freeze cycle in fairly close proximity to the freezing front. The 140 cm Petur cell, on the other hand, did not indicate any pressure changes and remained some distance from the freezing front for the duration of the experiment.

Figure 3.25 shows the soil pressure values beneath the pipe in the silt at 0.85 m from the sand-silt transition. The patterns shown are very similar to those observed near the B-B cross-section (4.3 m from transition), however, the pressure levels are much higher since pipe displacement is quite constrained.

Figure 3.25

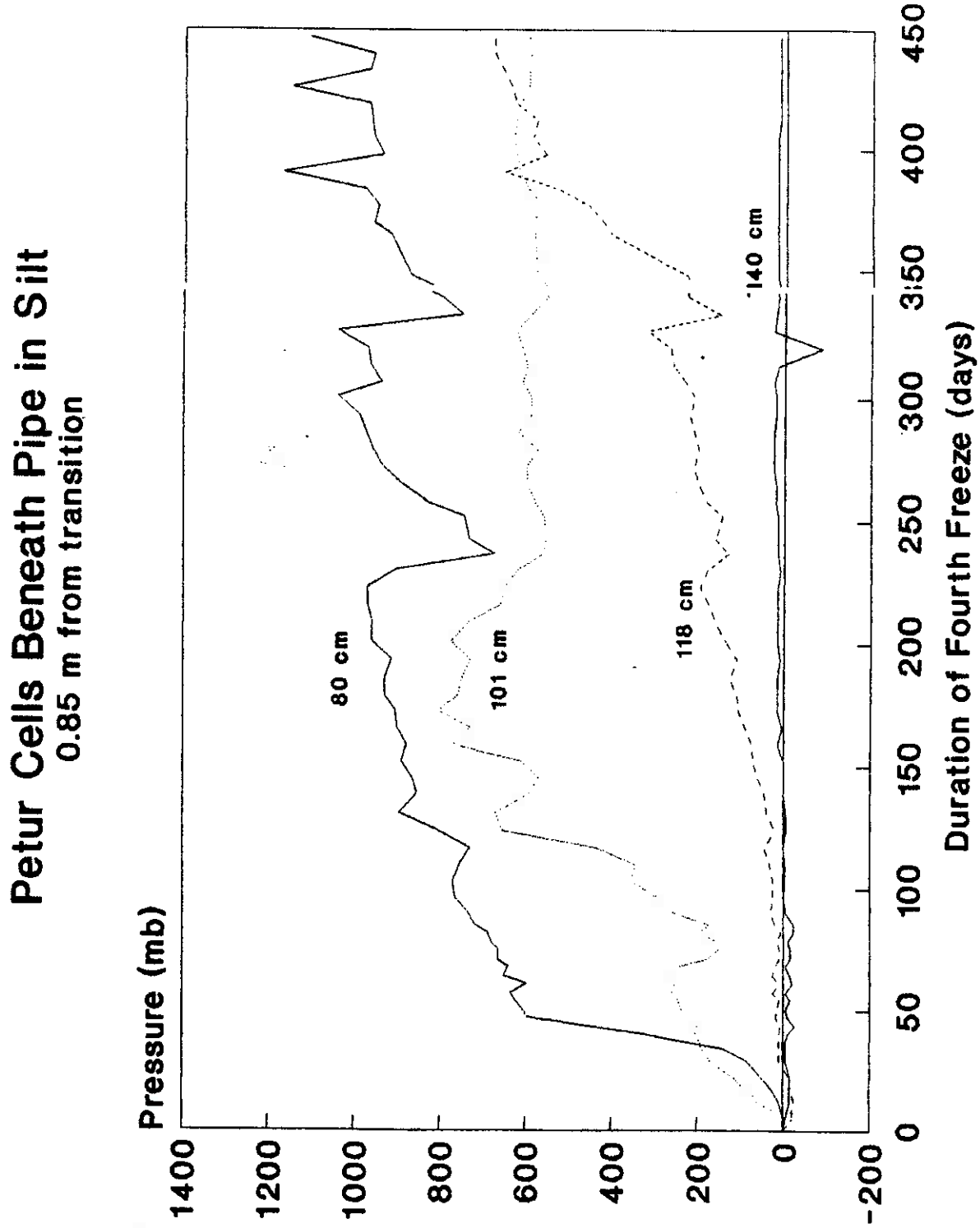
Petur Cells Beneath Pipe in Silt
0.85 m from transition
Pressure (mb)
1400
1200
1000
800
600
400
200
0
-200
0
50
100
150
200
250
300
350
400
450
Duration of Fourth Freeze (days)
80 cm
101 cm
118 cm
140 cm

Figure 3.26 shows the pressure values recorded at 2.35 m from the transition in the silt section for two cells placed 10 cm and 20 cm beneath the gap under the pipe (gap size about 7 cm). The recorded pressure levels are intermediate to those found at 4.3 m and 0.85 m for comparable depths (e.g. 80 cm cell in figures 3.24 and 3.25).

A similar placement was made in the sand section at 2.35 m, however, there is no gap between the pipe and the soil. The observations are shown in Figure 3.27 and differ from those of the silt section in that no pressure changes were noted until about day 160 even though the sand was frozen to a considerable depth by this date (it should be noted that the 10 cm cell appears to have failed completely). Since little heave occurs at this location, the response is probably due to pressure exerted on the soil by the pipe.

Figure 3.28 shows soil pressures measured near magnet heave site 4 (1 m off pipe axis and 3.4 m from transition). The temperatures at this site are largely controlled by ambient conditions with the coldest temperature being about -0.6 C in the near surface. This figure shows that there is a steady increase in soil pressure for the 45 cm sensor up to about day 150 and a gradual decline afterwards (the soil pressure is 485 mb on this date and the sensor and the 0 C isotherm are at about 54 cm). This decline in soil pressure was not noted at other sites where temperatures are colder and may reflect the differences in the creep properties between sites. The 75 cm sensor at this site

Figure 3.26

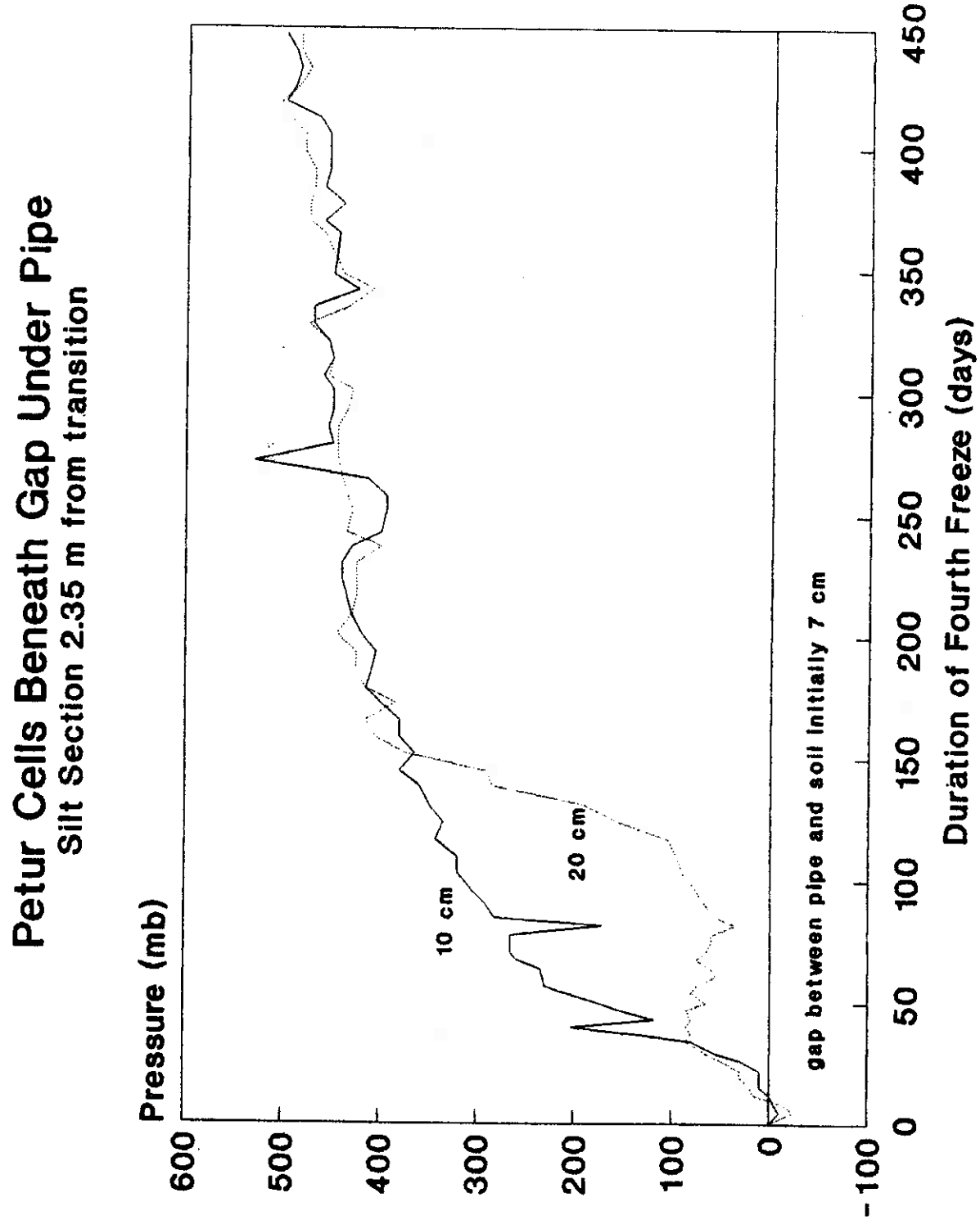
Petur Cells Beneath Gap Under Pipe
Silt Section 2.35 m from transition
Pressure (mb)
600
500
400
300
200
100
0
-100
0
50
100
150
200
250
300
350
400
450
Duration of Fourth Freeze (days)
10 cm
20 cm
gap between pipe and soil initially 7 cm

Figure 3.27

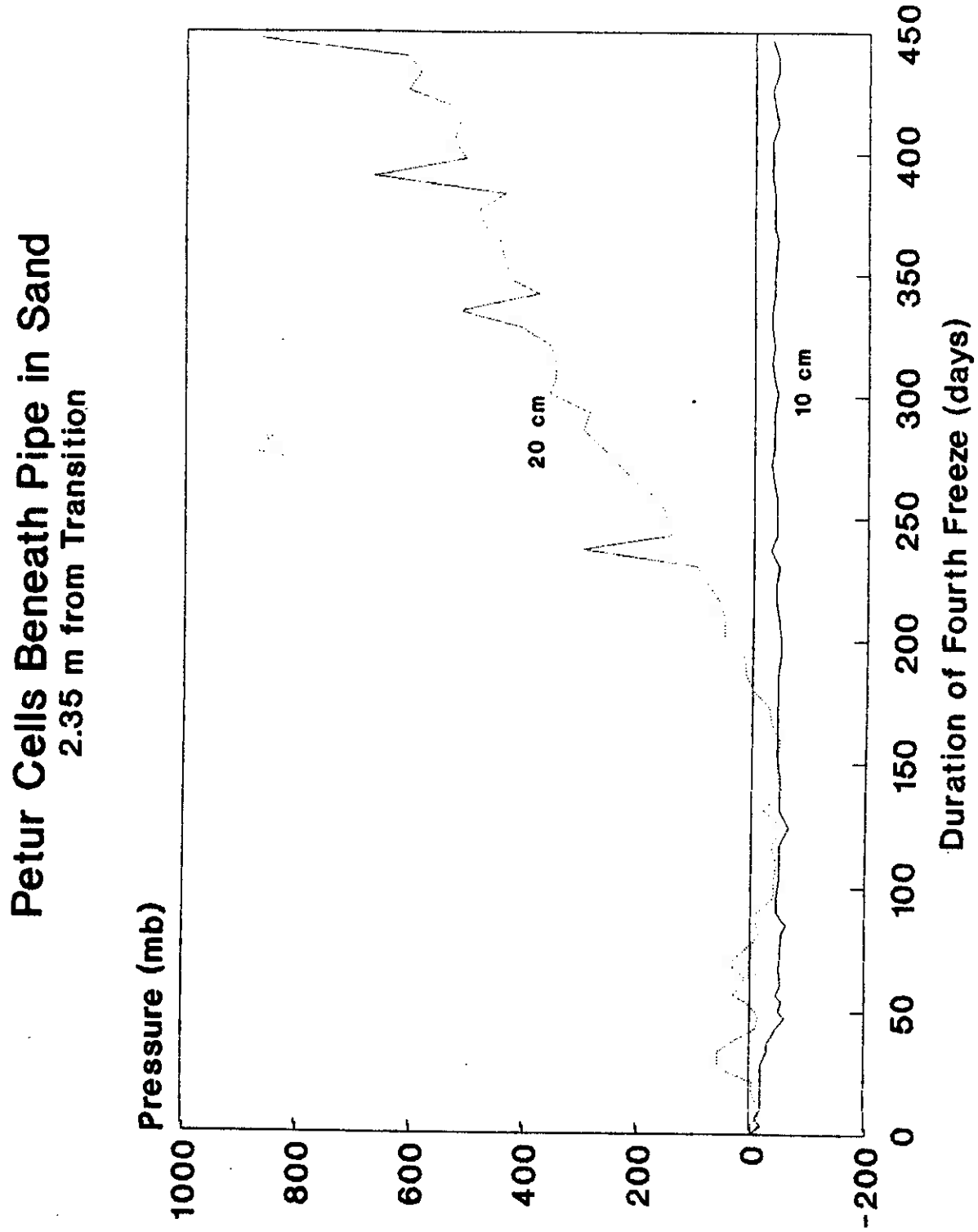
Petur Cells Beneath Pipe in Sand
2.35 m from Transition
Pressure (mb)
1000
800
600
400
200
0
-200
0
50
100
150
200
250
300
350
400
450
Duration of Fourth Freeze (days)
20 cm
10 cm

Figure 3.28

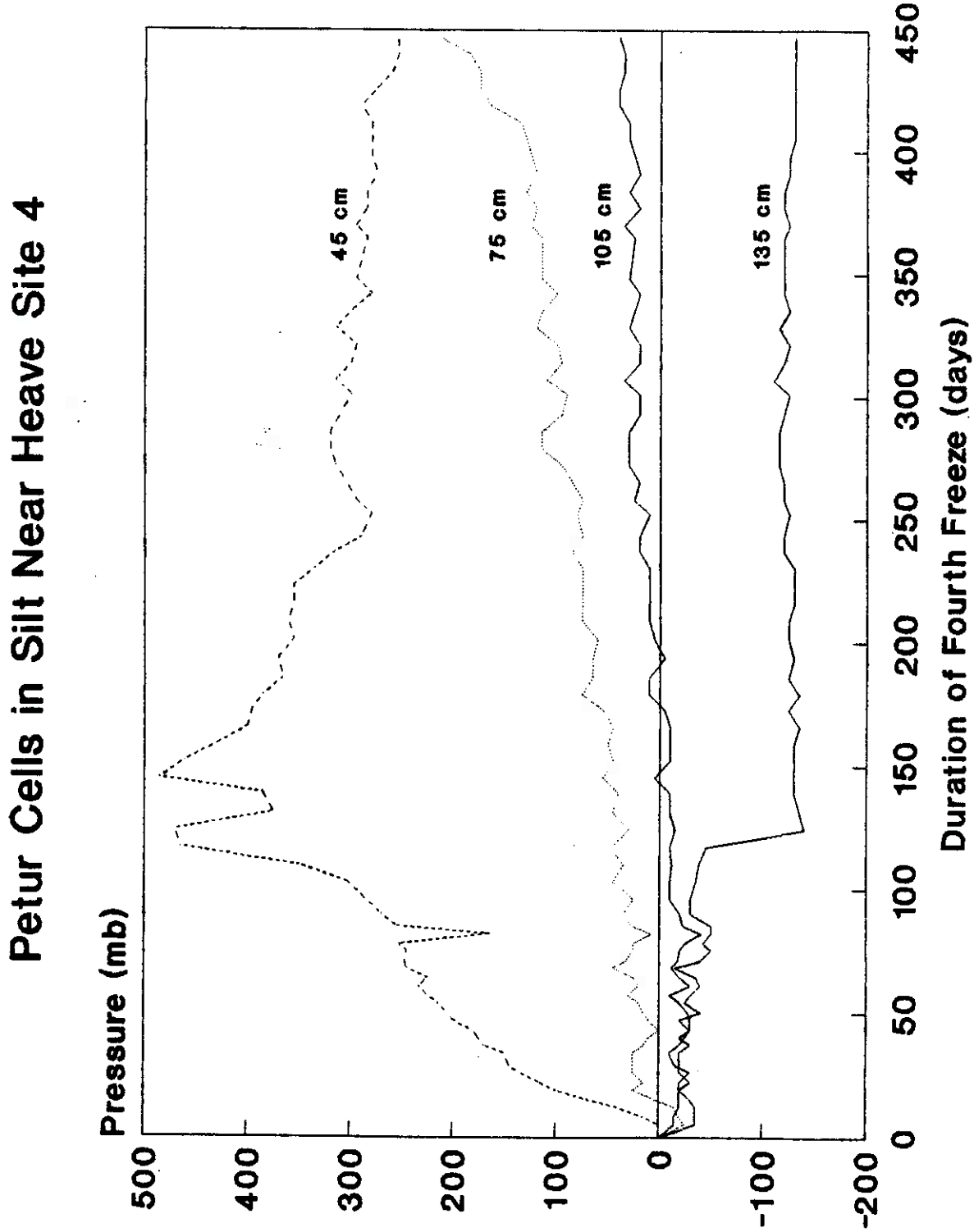
Petur Cells in Silt Near Heave Site 4
Pressure (mb)
500
400
300
200
100
0
-100
-200
0
50
100
150
200
250
300
350
400
450
Duration of Fourth Freeze (days)
45 cm
75 cm
105 cm
135 cm

also exhibited a very gradual increase in pressure during the course of the freeze cycle even though the 0 C isotherm never reached the sensor. The 105 cm sensor on the other hand remains largely unchanged while the 135 cm sensor showed an inexplicable sudden drop on day 120, remaining constant thereafter.

Directional Petur cells were also installed at selected sites. The Petur cells were designed to measure either total pressure (rubber bulb fully exposed to the soil), lateral pressure (rubber bulb only partially exposed to the soil positioned parallel to the isotherms) or downward pressures (cell's bulb exposed so that it faces the soil surface and should be recording pressures in a downward direction).

Figure 3.29 shows the pressure changes since Day 0 recorded at the 101 cm depth near the B-B cross-section along the pipe axis (see Figure 3.24) using these three different sensor designs. In general, the three sensors begin to show marked pressure increases on about day 125 before the 0 C isotherm has reached their position. The cells are within frozen ground by about day 225 and the pressure values are reasonably similar until about day 275 when the pressure values for the lateral and downward cells begin to decline with the latter showing the more rapid changes.

A similar configuration was used at the site located along the pipe axis 85 cm from the sand-silt transition (see Figure 3.25). This site is very close to magnet heave site 8. As above, the directional sensors are located at the 101 cm depth to

Figure 3.29

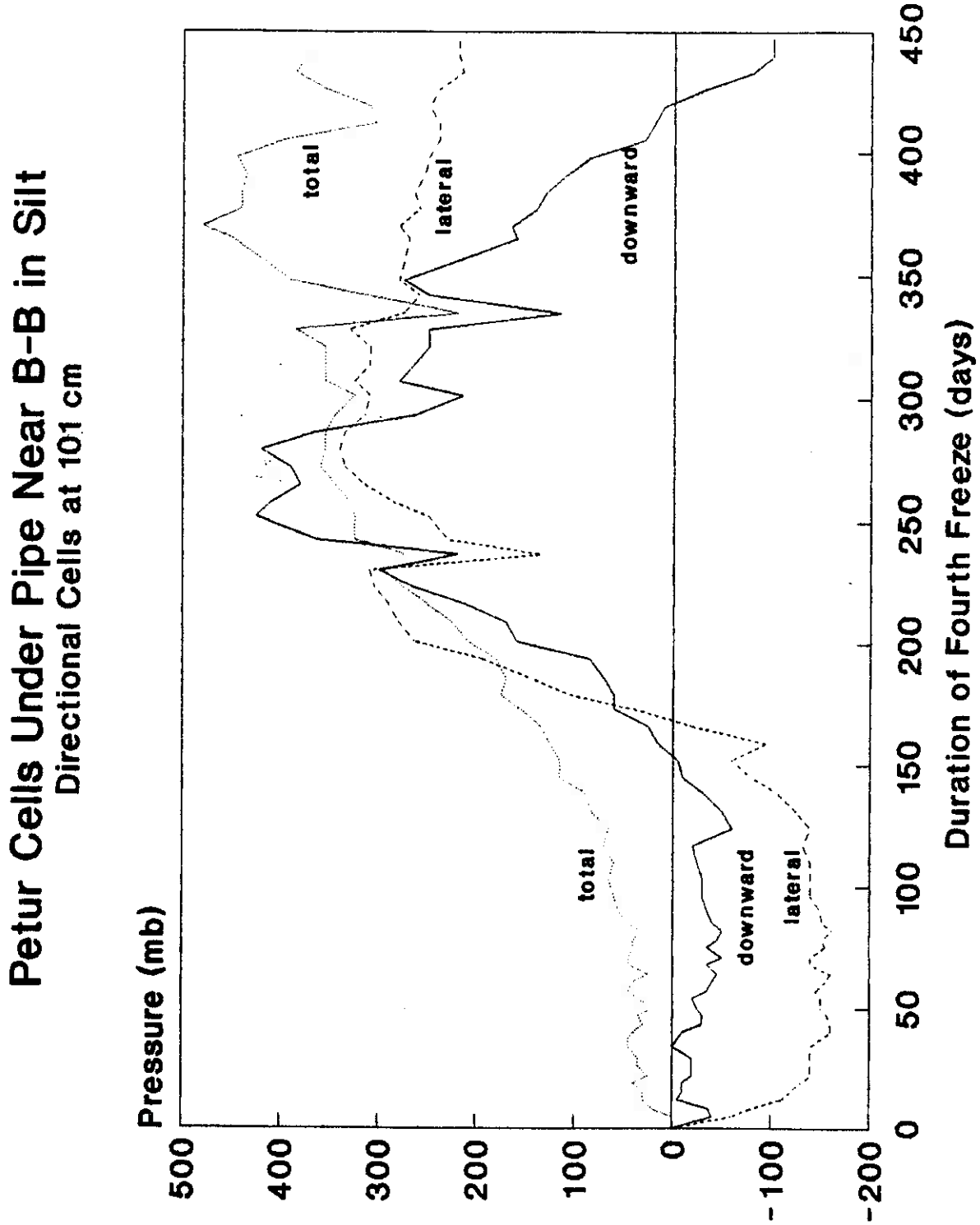
Petur Cells Under Pipe Near B-B in Silt
Directional Cells at 101 cm
Pressure (mb)
500
400
300
200
100
0
-100
-200
0
50
100
150
200
250
300
350
400
450
Duration of Fourth Freeze (days)
total
lateral
downward
total
downward
lateral

compliment the total pressure cell. The total and downward cells begin to show pressure increases soon after the freeze commences (Figure 3.30). By Day 100 the downward cell is still within unfrozen ground and the pressure level shows a precipitous drop and the lateral cell begins to rise. By Day 175, the cells are all within frozen ground.

3.7.2 Glotzl Cells

Glotzl cells have been used to measure soil pressures since the first freeze cycle. Cells are installed at 10, 46 and 86 cm beneath the pipe at the A-A and B-B cross-sections in the sand and silt respectively. Figures 3.31 and 3.32 show the pressure change measurements obtained for the silt and sand sections. The pressure levels for the 10 cm cells rise much more slowly and to a lower level in the silt section than in the sand.

The 10 cm cell in the silt section (Figure 3.31) is within frozen ground by about Day 30 and rises steadily to about Day 225; a plateau is reached and by day 325 the pressure levels begin to fall. Frost penetration at this site does not reach the 46 cm cell and no pressure changes are noted. The Petur cells located at this site (See Figure 3.24) serve to complement the Glotzl cells. The 80, 101, 118 and 140 cm Petur cells are about 20, 40, 60 and 80 cm beneath the pipe (assuming the base of the pipe to be about 60 cm from the soil surface). It is interesting to note that the differences in pressure observations using the two devices. The 80 cm Petur cell rises more rapidly than does

Figure 3.30

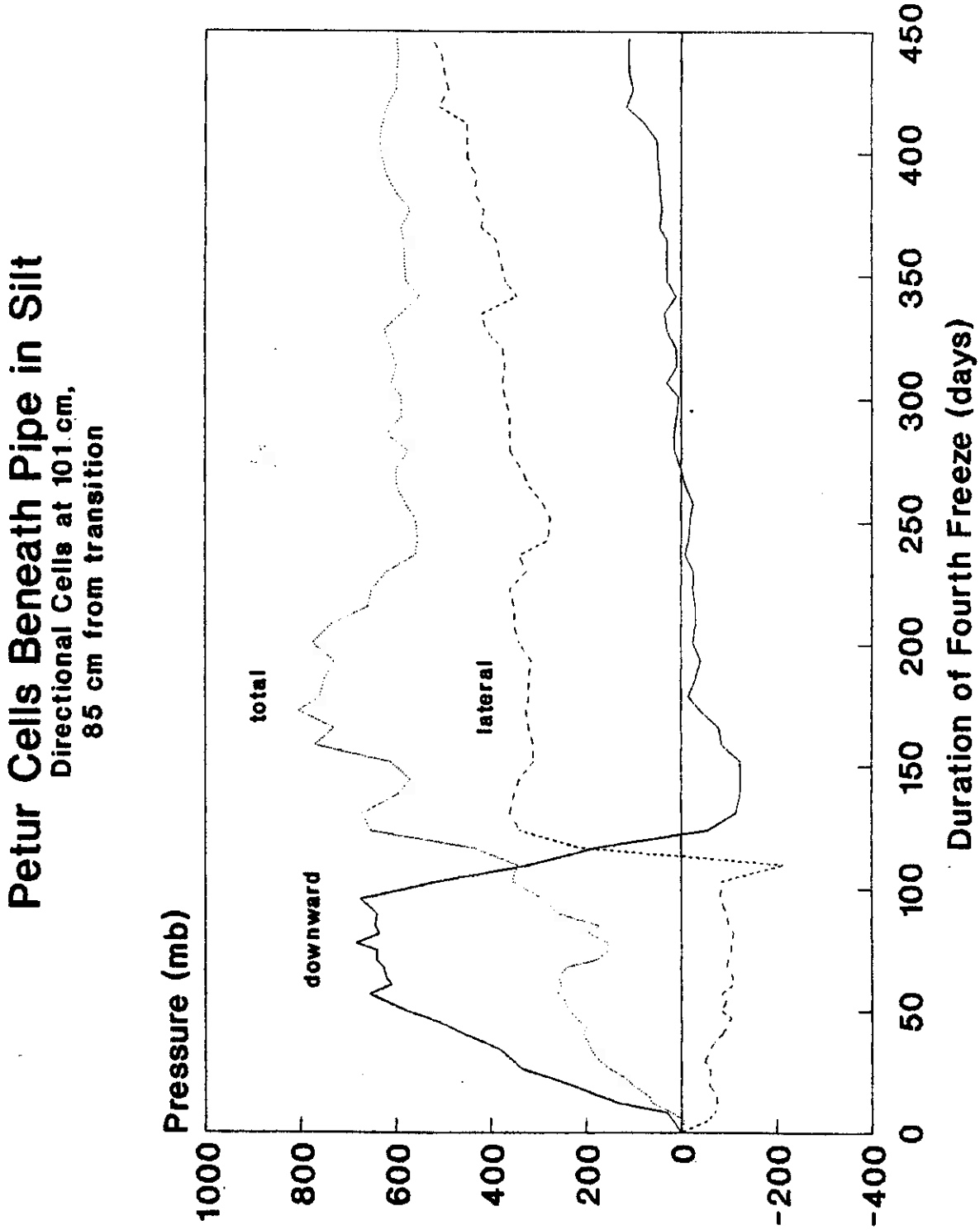
Petur Cells Beneath Pipe in Silt
Directional Cells at 101 cm,
85 cm from transition
Pressure (mb)
1000
800
600
400
200
0
-200
-400
total
downward
lateral
0
50
100
150
200
250
300
350
400
450
Duration of Fourth Freeze (days)

Figure 3.31

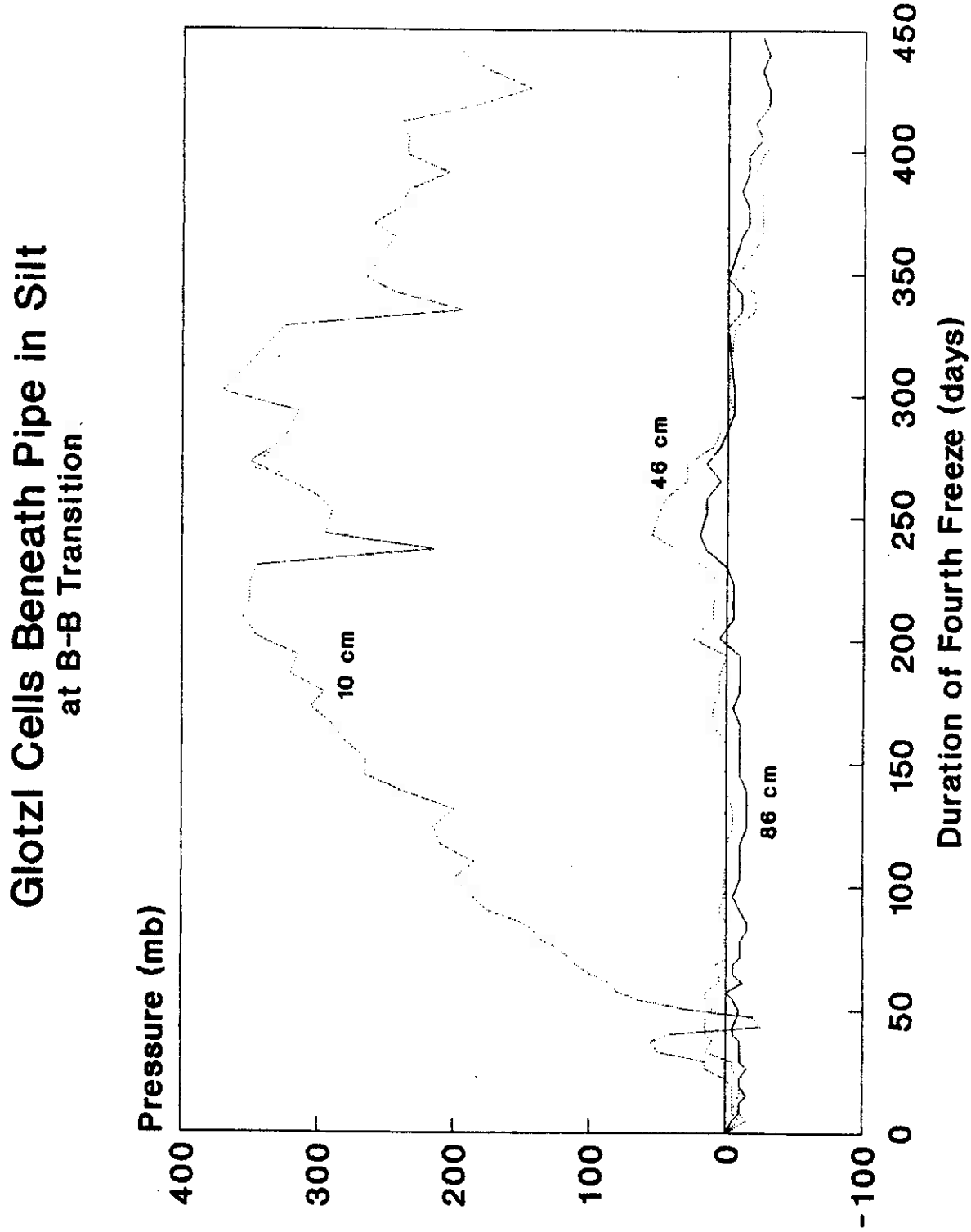
Glotzl Cells Beneath Pipe in Silt
at B-B Transition
Pressure (mb)
400
300
200
100
0
-100
0
50
100
150
200
250
300
350
400
450
Duration of Fourth Freeze (days)
10 cm
46 cm
86 cm

Figure 3.32

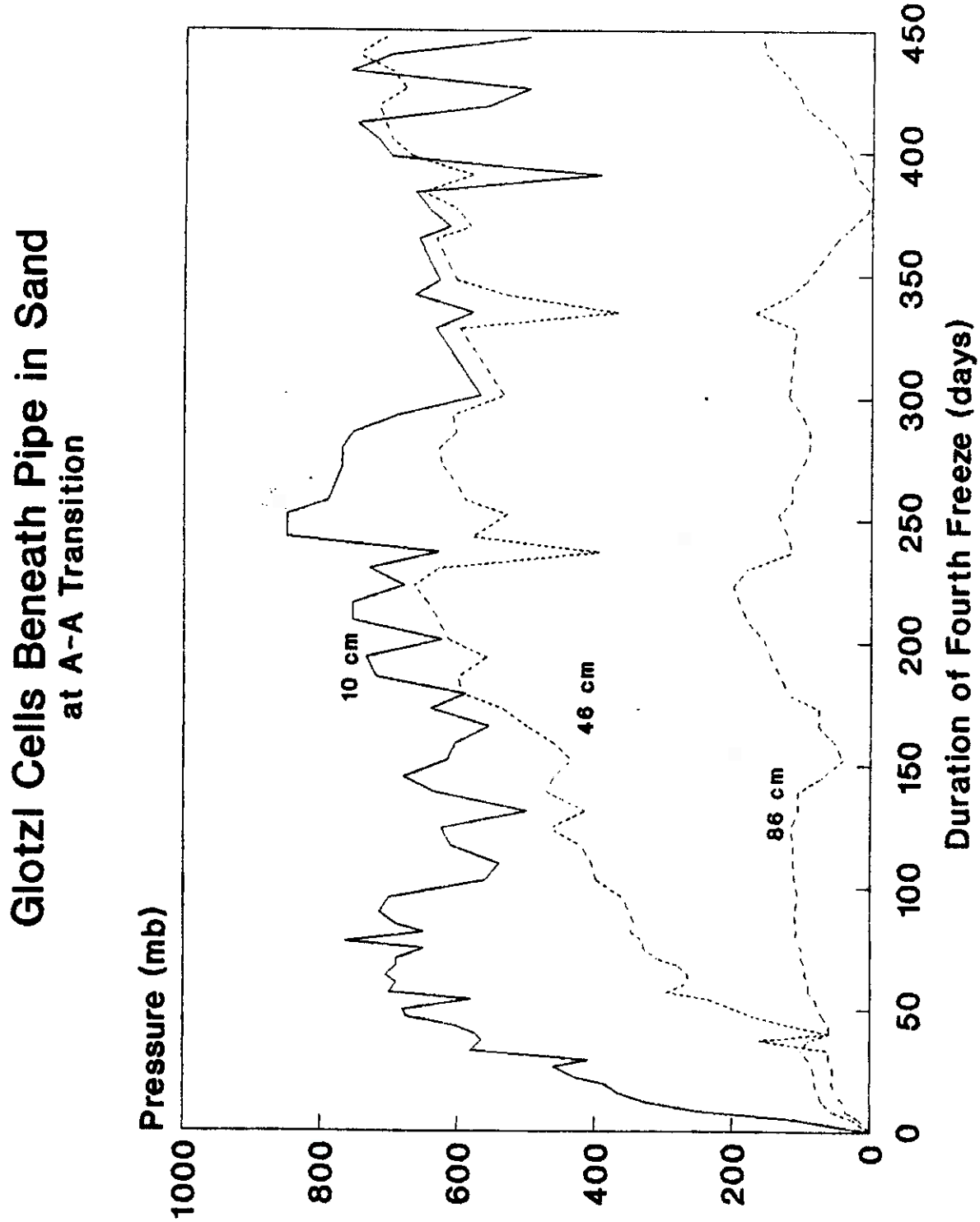
Glotzl Cells Beneath Pipe in Sand
at A-A Transition
Pressure (mb)
1000
800
600
400
200
0
10 cm
46 cm
86 cm
0
50
100
150
200
250
300
350
400
450
Duration of Fourth Freeze (days)

the comparable 20 cm Glotzl cell and does not exhibit the pressure decrease that this cell does (see Figures 3.24 and 3.31). Also, the 101 cm Petur cell exhibits pressure increases while the 46 cm Glotzl does not. It is possible that the pressure sensing devices differ in their response or that real differences in soil conditions exist within short distances. In order to resolve these apparent discrepancies, a comparison will be made between the two types of cells prior to the 5th freeze. Also, thermistors will be attached near the sensing end of each cell so that the thermal-pressure conditions at a given point in time are known.

3.9 Surface Levelling

The shape of the soil surface is recorded by optical survey of a grid of fixed points on the soil surface (0.5 m and 1 m apart) approximately once per month (less frequently toward the end of the freeze cycle). Manipulation of this data can reveal features of the spatial and temporal variation of the soil behaviour during the experiment. In this section, results for three simple manipulations of the surface heave data are presented:

- Changes to the configuration of the surface after each freeze - thaw cycle.
- Total heave, or the change in elevation from the start of the freeze cycle.
- The changing spatial distribution of the rate of heave over time.

3.9.1 Surface changes between cycles.

Changes to the soil structure may be inferred from permanent changes to the configuration of the surface after each freeze - thaw cycle. Figure 3.33 shows the soil surface following the period of thaw settlement for the first, second, and third cycles of the experiment. With each cycle, the ground surface has become increasingly uneven, with a total relief of over 10 cm after the third freeze cycle. The increasing relief is the cumulative effect of several processes, including frost heave, thaw settlement, and the mechanical stresses imposed by the pipe.

Ice segregation leads to consolidation of the soil. The caen silt, initially uniform and without structure, has become consolidated over the freeze-thaw cycles, so that the silt has become progressively lower relative to the sand. Within the silt, the consolidation is greatest adjacent to the pipe, where freezing has penetrated furthest into the soil.

Consolidation of the silt is apparent to a lesser extent at the margins of the experiment, despite the limited depth of freezing there. This is a result of water being drawn to the annulus of freezing soil around the pipe. The soil becomes increasingly consolidated toward the pipe axis, where the suction forces are actually generated. In the longitudinal direction, consolidation is greatest at the sand-silt transition.

The mechanical forces acting on the pipe have caused the pipe to become permanently deformed, as mentioned elsewhere in

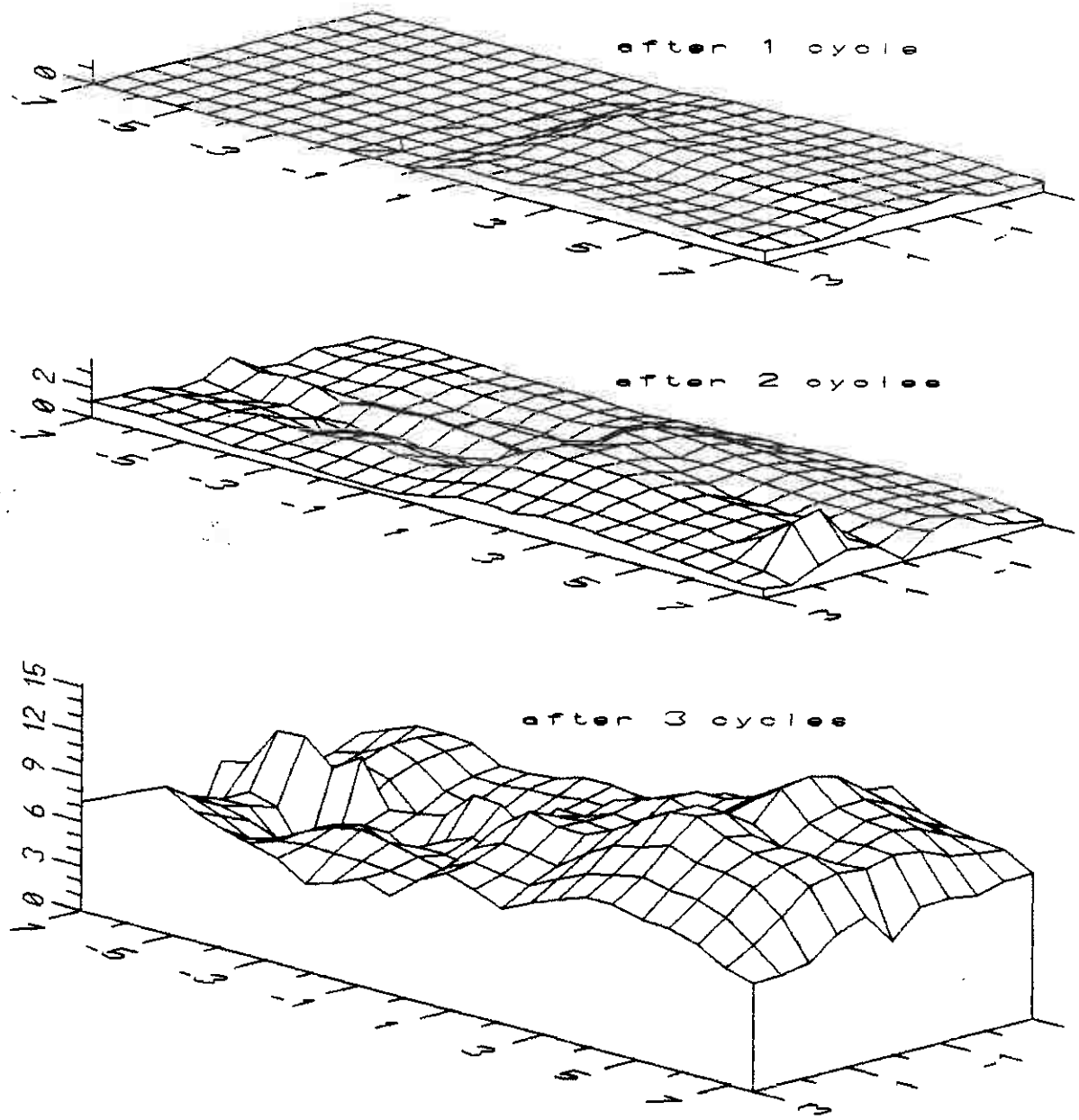

Figure 3.33 Soil surface between freeze cycles.
Vertical exageration 1:500.

the report. This has resulted in some jacking of the pipe out of the ground in the silt section, as evident in the ridge raised along the pipe axis. In the sand section, downward pressure of the pipe on the sand is evident, with a slight depression forming along the pipe axis in the sand section.

3.9.2 Total Heave during the fourth freeze cycle.

Total heave over the surface for a given freeze cycle can be extracted from the survey data, by examining the change in elevation from the start of the freeze. As the surface becomes increasingly uneven between cycles, the shape of the surface during a freeze cycle is less a record of the actual pattern of frost heave during the cycle than a cumulative history of the segregation/consolidation and thaw settlement that has occurred from the beginning of the experiment. Figure 3.34 shows the total heave of the surface for different dates of the freeze cycle. Because the heave rate declines rapidly with time (see below), the surface configuration which develops in the early freezing stages are not greatly altered over the extended freezing period. The dominant feature is the higher rate of heave adjacent to the pipe in the silt section. Almost no heave takes place in the sand, except directly adjacent to the pipe. The plot indicates some uplift in the sand adjacent to the pipe and near the transition. Excavation in this area at the conclusion of the experiment will yield information on the processes which have occurred in this area.

Figure 3.34 Surface heave from levelling data. Heave is calculated as change in surface elevation from day -2. Vertical exaggeration 200:1.

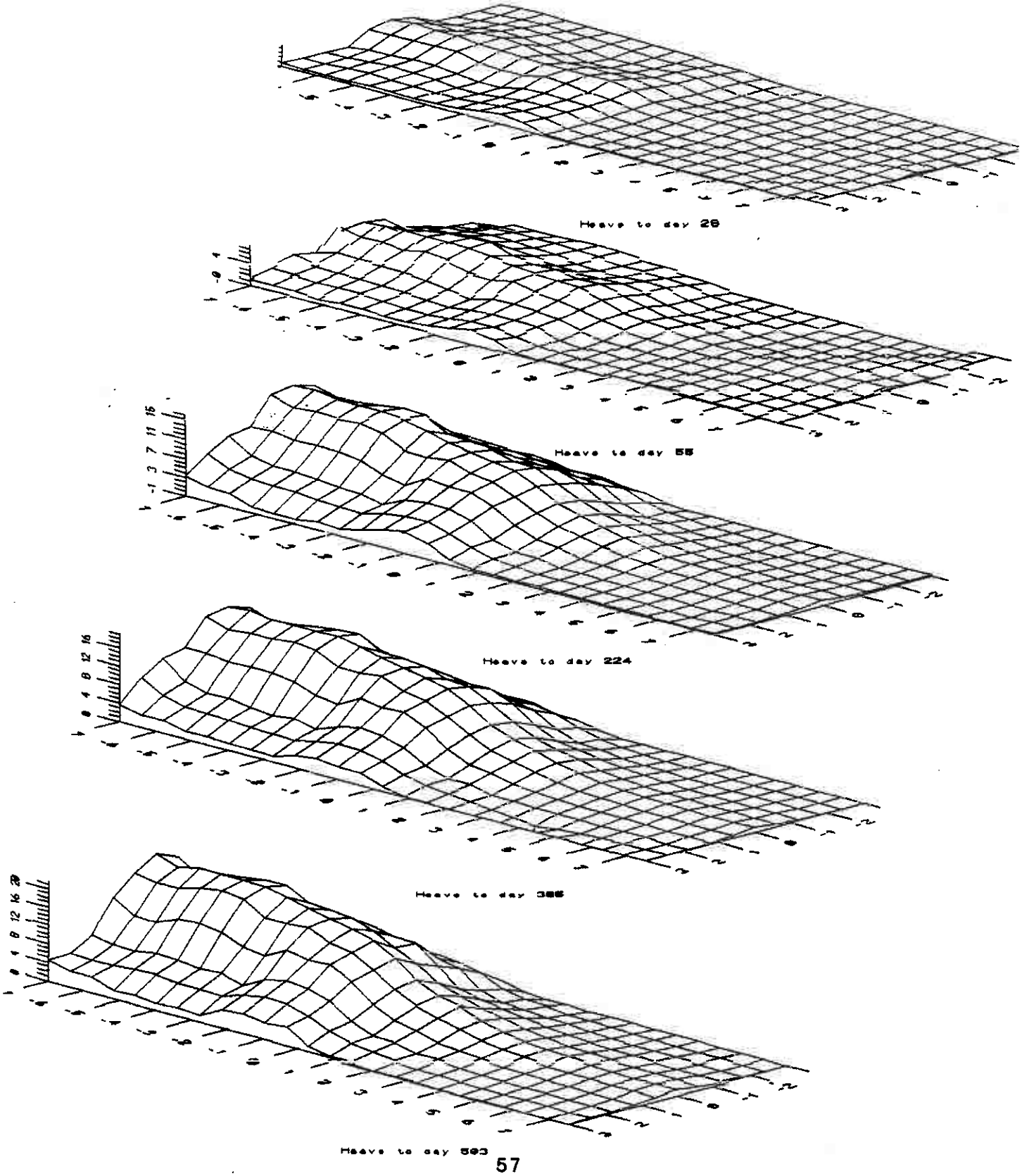

Comparison of the "heave surface" for day 503 of the freeze (the bottom diagram of figure 3.34) and the actual soil surface (Figure 3.35) for that day shows that frost heave behaviour near the pipe varies fairly smoothly, despite the abrupt change in the slope of the surface above the pipe.

Calculation of the total volume of heave from the start of the freeze cycle shows approximately 5 cubic meters of heave from day 0 to day 503. This represents an average heave of 6 cm over the whole surface.

3.9.3 Heave rates over time.

The changing spatial distribution of the rate of heave over time can be calculated by examining elevation changes between dates within the survey record. Figure 3.36 shows the spatial variation in heave rate calculated for different periods of the freeze cycle. The dominant features of the series are the higher rate of heave adjacent to the pipe in the silt section, and the generally decreasing heave rate as the freeze cycle progresses.

The heat sink effect of the pipe becomes less localized as the freezing front becomes progressively deeper, with the result that the initially concave heave-rate surface in the silt section becomes convex by the period shown in the middle of the series. The same sort of transition occurs very rapidly (between the first two periods shown) in the sand section. By the middle period shown, almost all of the sand section shows a slightly negative elevation change (the line on the surface which is not

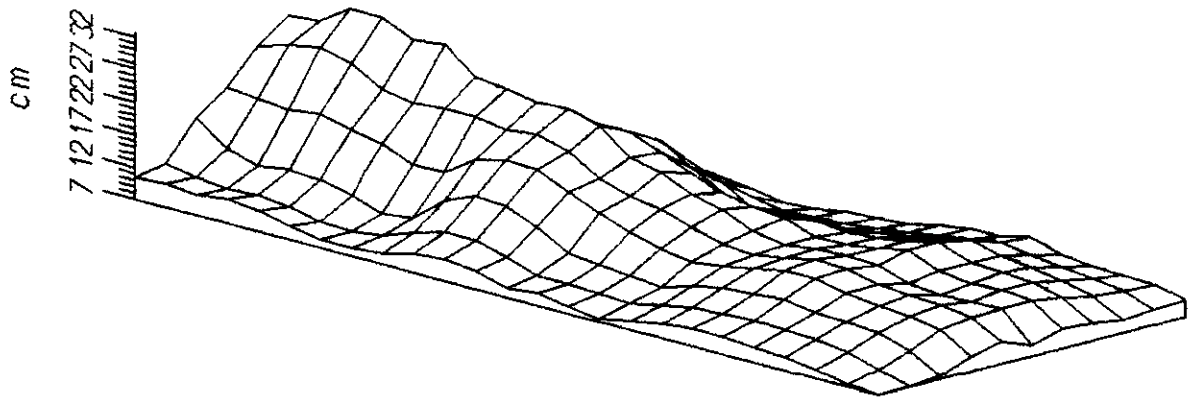

Figure 3.35 Soil surface on day 503 of fourth freeze. Vertical exageration 1:200.

Figure 3.36 Surface variation in heave rate over time. Graduations on the vertical scale represent 0.05 mm/day. The line on the surface which is not part of the grid is the line of zero rate of heave.

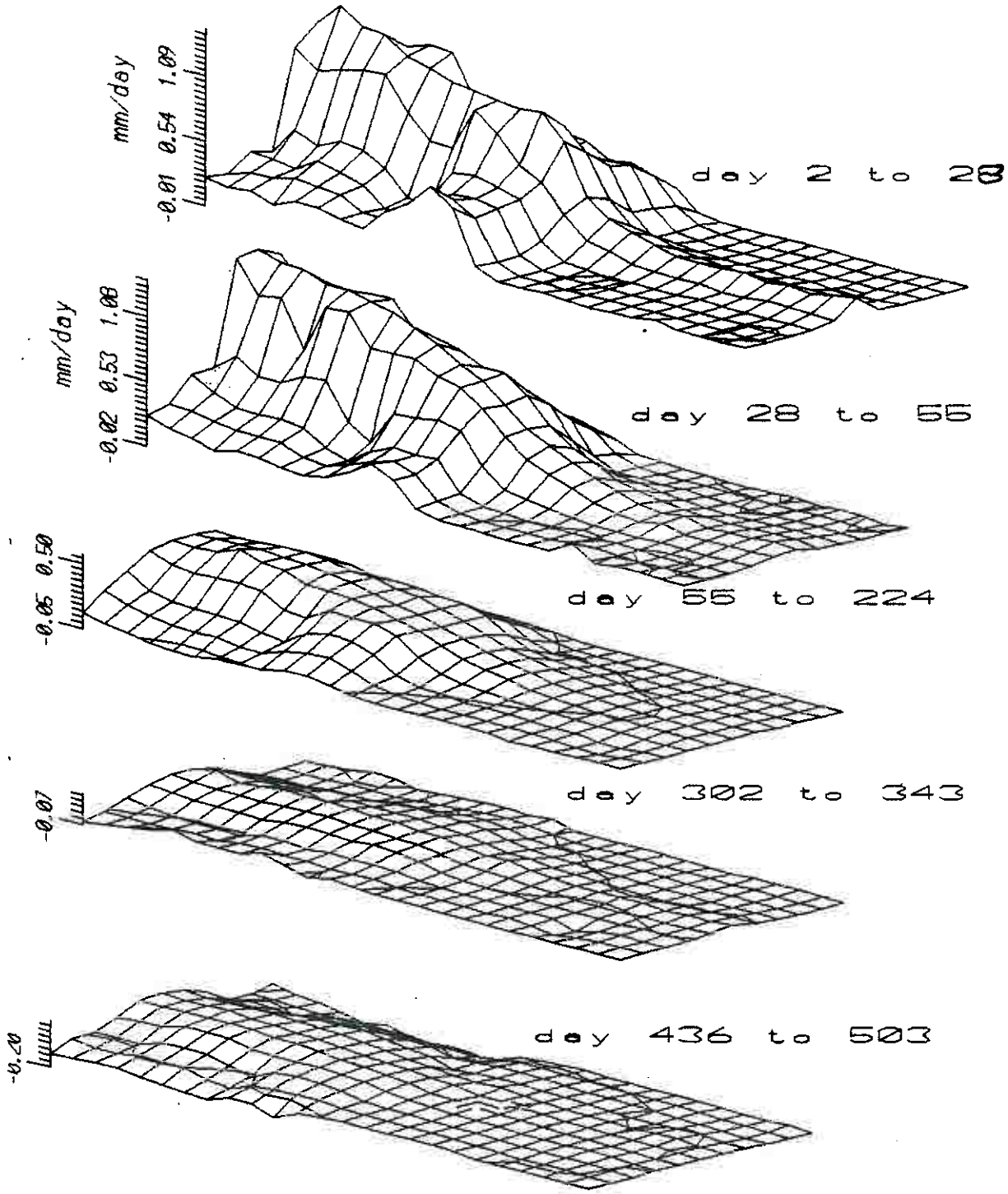

part of the x-y grid is the line of zero heave rate).

In the initial stages, the heave rate is augmented along the sand-silt transition. The higher frost penetration rate and greater availability in the sand, and the availability of water from the sand probably account for this. Consolidation of the silt as a result of water being drawn toward the transition zone may also account for the depressed heave rate in the silt near the pipe and adjacent to the silt-sand transition.

After day 300, the heave rate in the silt away from the pipe is low or negative, again due in part to the movement of water within the soil toward the freezing annulus around the pipe.

References

Blanchard, D. and M. Fremond. 1985. Soils frost heaving and thaw settlement, Proceedings of the 4th International Symposium on Ground Freezing, pp. 209-216.

Geotechnical Science Laboratories, 1982. Feasibility studies for stresses in a pipeline buried in freezing soil. Report to Energy, Mines and Resources, Canada, Earth Physics Branch. 36 pp.

Geotechnical Science Laboratories, 1983. Investigation of soil freezing in association with a buried chilled pipeline in a large-scale test facility, Phase 2. 41 pp.

Geotechnical Science Laboratories, 1984a. Analysis of stresses developed in pipelines buried in freezing ground. Report to Energy, Mines and Resources, Canada, Earth Physics Branch, 59 pp.

Geotechnical Science Laboratories, 1984b. Experimentation sur le gel d'un sol et d'une canalisation enterree et refroidie dans une installation d'essai de grandes dimensions 3e phase. Rapport pour le Ministere de l'Energie, Mines et Resources, Direction de la Physique du Globe. 73 pp.

Geotechnical Science Laboratories, 1985. Analyses of stresses developed in pipelines buried in freezing ground. Final report for Earth Physics Branch, Energy, Mines and Resources, 39pp.

Geotechnical Science Laboratories, 1988. The Third Freeze Cycle of the Canada-France Ground Freezing Experiment. Final report for Earth Physics Branch, Energy, Mines and Resources

Konrad, J.-M. and N.R.Morgenstern. 1981. The segregation potential of a freezing soil. Canadian Geotechnical Journal, 18: 482-491.

Ladanyi, B. 1983. Shallow foundations on frozen soil: Creep settlement, Journal Geotechnical Engineering, ASCE, Vol. 109, No. 11, pp. 1434-1448.

Miller, R.D. 1972. Freezing and heaving of saturated and unsaturated soils, Highway Research Record, Vol. 393, pp. 1-11.

Penner, E. 1986. Aspects of ice lens growth in soils, Cold

Regions Science and Technology, Vol. 13, No. 1, pp. 91-100.

Shen, M. and B. Ladanyi 1987. Modelling of coupled heat, moisture and stress field in freezing soil, Cold Regions Science and Technology, Vol. 14, No. 3, pp. 237-246.

Shen, M. and B. Ladanyi, 1988. Calculation of stress field in soil during freezing. Procedings of the 5th International Symposium on Ground Freezing.

Smith, M.W. and D.E. Patterson 1989. Detailed observations on the nature of frost heaving at a field scale, Canadian Geotechnical Journal, Volume 26, No. 2, pp. 306-312.

Appendix I

Use of boundary-fitted Curvilinear Coordinate Systems in connection with chilled pipeline design.

USE OF BOUNDARY-FITTED CURVILINEAR COORDINATE SYSTEMS IN CONNECTION WITH CHILLED PIPELINE DESIGN

Mu Shen and Branko Ladanyi
CINEP, Ecole Polytechnique de Montreal
Montreal, H3C 3A7, CANADA

INTRODUCTION

For designing chilled pipelines and other structures in cold regions, numerical techniques are useful and essential for calculating the depth of freeze and thaw penetration. Because of certain numerical difficulties, some powerful finite difference techniques usable for one dimensional problems (Goodrich,1977) can not be extended to multidimensional and irregularly shaped domains.Up to now,the majority of simulations of such problems in the literature have been carried out using the finite element method. The finite element methods can be usually separated into two groups: methods with a moving interface (Hwang,1972; O'Neill & Lynch,1983) and methods without the free boundary, based on use the apparent heat capacity,freezing index or enthalpy (Comini et al.,1974;Blanchard & Fremond,1984; Cames-Pintaux and Nguyen-Lamba,1986).

For long-term computations, a high numerical efficiency is required for minimizing costs. The finite difference method requires normally much smaller memory and amount of calculation than the finite element method, which is important when using a personal computer or a small computer system to simulate such problems.In this paper,the Alternating Direction Implicit(ADI) difference method and a boundary fitted curvilinear coordinate system are used to determine thaw penetration within a two-dimensional road embankment cross-section.The calculated results are compared with actual measured data. All programs have been implemented on an IBM personal computer.

GRID GENERATION

In the past decade, the numerical generation of curvilinear

coordinate systems has provided the powerful tool for the development of finite difference solutions of partial differential equations in regions with arbitrarily shaped boundaries. Although this method has been developed from computational fluid dynamics and aerodynamics, the techniques are equally applicable to heat and mass transfer problems in cold regions, and to other areas.

Normally, the procedures for generation of curvilinear coordinate systems may be separated into two types: (1) numerical solution of partial differential equations, e.g. elliptic or hyperbolic generation systems; (2) construction by algebraic interpolation. In this paper,the grid was generated by the coupled Poisson's equations (Thompson, et al.):

[1.A] $$\xi_{xx} + \xi_{yy} = P(\xi,\eta)$$

[1.B] $$\eta_{xx} + \eta_{yy} = Q(\xi,\eta)$$

The source terms P and Q can control the spacing and orientation of the coordinate lines. However, the forms of the source terms require artful selection and depend on the problem.Thomas and Middlecoff(1980) suggested for the source terms to have the form:

[2.A] $$P(\xi,\eta) = \phi(\xi,\eta)\cdot(\xi_x^{\,2} + \xi_y^{\,2})$$

[2.B] $$Q(\xi,\eta) = \psi(\xi,\eta)\cdot(\eta_x^{\,2} + \eta_y^{\,2})$$

in which the functions ϕ,ψ on the boundaries are defined as

[3.A] $$\phi = -\frac{x_\xi x_{\xi\xi} + y_\xi y_{\xi\xi}}{x_\xi^{\,2} + y_\xi^{\,2}} \qquad \text{on boundaries } \eta = \text{const}$$

[3.B] $$\psi = -\frac{x_\eta x_{\eta\eta} + y_\eta y_{\eta\eta}}{x_\eta^{\,2} + y_\eta^{\,2}} \qquad \text{on boundary } \xi = \text{const}$$

Once the function ϕ is defined at each point of the horizontal boundaries η=const in the considered domain,its value at interior mesh points can be calculated by linear interpolation along vertical mesh lines ξ = const. Similarly, ψ is computed by interpolation along the horizontal mesh lines η=const between

the boundaries.

Substituting(2) into(1),and transforming it to ξ,η coordinates by interchanging the roles of dependent and independent variables, yields a quasilinear elliptic system of equations:

[4.A] $$g_{22}(x_{\xi\xi} + \phi x_{\xi}) - 2g_{12}x_{\xi\eta} + g_{11}(x_{\eta\eta} + \psi x_{\eta}) = 0$$

[4.B] $$g_{22}(y_{\xi\xi} + \phi y_{\xi}) - 2g_{12}y_{\xi\eta} + g_{11}(y_{\eta\eta} + \psi y_{\eta}) = 0$$

with

[5.A] $$g_{11} = x_{\xi}^{2} + y_{\xi}^{2}$$

[5.B] $$g_{12} = x_{\xi}x_{\eta} + y_{\xi}y_{\eta}$$

[5.C] $$g_{22} = x_{\eta}^{2} + y_{\eta}^{2}$$

The equations (4) are solved by SLOR iteration in the rectangular computational domain to generate the grid in the physical domain.This method of evaluating the parameters ϕ and ψ insures that the grid distribution throughout the interior of the domain will be governed by grid point distribution assigned on the boundaries, and that the grid lines will be locally orthogonal to the boundaries.

Figures (1) and (2) show the non-stretching and stretching meshes in chilled pipeline embankment generated by the above generation system. These grid meshes have smooth and regular character, and guarantee the preservation throughout the domain of the grid point distribution specified on the boundaries. The grid meshes were generated using a IBM-PC-AT personal computer, the consumed time for the each mesh is about 5 minutes.

HEAT TRANSFER EQUATION

In most cases, the heat flow in soils from thermal vapor transfer is much smaller than from thermal conduction. The heat

transfer for two-dimensional problems may be written as:

$$[6] \quad \overline{C}\cdot\frac{\partial T}{\partial t} = \frac{\partial}{\partial x}\left(\overline{\lambda}\cdot\frac{\partial T}{\partial x}\right) + \frac{\partial}{\partial y}\cdot\left(\overline{\lambda}\cdot\frac{\partial T}{\partial y}\right)$$

where x,y — space coordinates (m); T — soil temperature (^{0}C); t — time(sec); $\overline{C}$ — apparent heat capacity(J/m^3/^{0}C); λ — apparent thermal conductivity (W/m/^{0}C). The apparent heat capacity and thermal conductivity functions can be approximated by

$$[7] \quad \overline{C} = \begin{cases} C^+ & \text{for unfrozen soil} \\ C^- + L\cdot\rho_d\cdot\dfrac{\partial Wu}{\partial T} & \text{for frozen soil} \end{cases}$$

$$[8] \quad \overline{\lambda} = \begin{cases} \lambda^+ & \text{for unfrozen soil} \\ \lambda^- & \text{for frozen soil} \end{cases}$$

where: Wu — unfrozen water content (kg/kg); L — latent heat of fusion (J/kg); and ρ_d — dry density of soil (kg/m^3)

The general forms of definite conditions may be written as follows:

(a) Initial condition:

$$[9] \quad f(x,y,0) = f(x,y)$$

(b) Boundary conditions:

$$[10] \quad T|_{\Gamma_1} = \chi_1(x,y,t)$$

$$[11] \quad \left.\frac{\partial T}{\partial n}\right|_{\Gamma_2} = \chi_2(x,y,t)$$

Usually, the relationship between unfrozen water content and temperature Wu=Wu(T) is defined by experiments.

When a general boundary-conforming curvilinear coordinate system is used in the solution of partial differential equations, the equations must first be transformed to the curvilinear coordinates. The transformed equations are of the same type as the original ones, but are more complicated in that they contain more terms and variable coefficients. The heat transfer equation

(6) transformed to the curvilinear coordinate system (ξ,η), can be written as:

$$[12] \quad g\cdot\overline{C}\cdot\frac{\partial T}{\partial t} = g_{22}\cdot\frac{\partial}{\partial\xi}\left(\overline{\lambda}\cdot\frac{\partial T}{\partial\xi}\right) - 2g_{12}\cdot\frac{\partial}{\partial\xi}\left(\overline{\lambda}\cdot\frac{\partial T}{\partial\eta}\right) + g_{11}\cdot\frac{\partial}{\partial\eta}\left(\overline{\lambda}\cdot\frac{\partial T}{\partial\eta}\right) + \tau\cdot\overline{\lambda}\cdot\frac{\partial T}{\partial\xi} + \sigma\cdot\overline{\lambda}\cdot\frac{\partial T}{\partial\eta}$$

with

$$[13.A] \quad \sigma = (y_\xi\cdot Dx - x_\xi\cdot Dy)/\sqrt{g}$$

$$[13.B] \quad \tau = (x_\eta\cdot Dy - y_\eta\cdot Dx)/\sqrt{g}$$

$$[13.C] \quad Dx = g_{22}\cdot x_{\xi\xi} - 2g_{12}\cdot x_{\xi\eta} + g_{11}\cdot x_{\eta\eta}$$

$$[13.D] \quad Dy = g_{22}\cdot y_{\xi\xi} - 2g_{12}\cdot y_{\xi\eta} + g_{11}\cdot y_{\eta\eta}$$

$$[13.E] \quad \sqrt{g} = x_\xi\cdot y_\eta - x_\eta\cdot y_\xi$$

where: $\sqrt{g}$ is the Jacobian; and g_{11}, g_{12}, g_{22} are covariant metric components, defined by the equations (5.A) and (5.B)

In the transformed ξ-η plane, the outward normal derivative of an arbitrary function T at the boundary of the region has the following forms:

$$[14.A] \quad \frac{\partial T}{\partial n} = \frac{1}{\sqrt{g}}\left(\sqrt{g_{22}}\cdot\frac{\partial T}{\partial\xi} - \frac{g_{12}}{\sqrt{g_{22}}}\cdot\frac{\partial T}{\partial\eta}\right) \quad \text{for constant } \xi$$

or

$$[14.B] \quad \frac{\partial T}{\partial n} = \frac{1}{\sqrt{g}}\left(\sqrt{g_{11}}\cdot\frac{\partial T}{\partial\eta} - \frac{g_{12}}{\sqrt{g_{11}}}\cdot\frac{\partial T}{\partial\xi}\right) \quad \text{for constant } \eta$$

If the ξ-η coordinates are locally orthogonal around the boundaries of interest, Eqs.(14.A) and (14.B) reduce simply to

$$[15.A] \quad \frac{\partial T}{\partial n} = \frac{\sqrt{g_{22}}}{\sqrt{g}}\frac{\partial T}{\partial\xi}$$

$$[15.B] \quad \frac{\partial T}{\partial n} = \frac{\sqrt{g_{11}}}{\sqrt{g}}\frac{\partial T}{\partial\eta}$$

Using the finite difference method and the curvilinear

coordinate system,a numerical analysis of temperature field in a thawing embankment in permafrost was carried out (Shen and Ladanyi,1989), and the simulated results were found to compare well with the actual measured data. We are presently using this method to simulate the temperature, moisture and stress fields around a chilled pipeline buried in a freezing soil.

REFERENCES

Blanchard,D. & Fremond,M.,1984, The Stefan problem:computing without the free boundary, Int. J. for Num. Methods in Engrg., Vol.20,pp.757-771.

Comes-Pintaux,A.M. & Nguyen-Lamba,M.,1986, Finite-element enthalpy method for discrete phase change,Num. Heat Transfer, Vol.9,pp.403-417.

Goodrich,L.E.,1978, Efficient numerical technique for one-dimensional thermal problems with phase change, Int. J. Heat & Mass Transfer, Vol.21, pp.615-621.

Shen,M. & Ladanyi,B.,1989,Numerical solutions for freezing and thawing of soils using boundary-fitted curvilinear coordinate systems,Proc.of Int.Sym. on Frost in Geotechnical Engineering.

Thompson,J.F. & Warsi,Z.U.A. & Mastin,C.W.,1985,Numerical grid generation -- foundations and applications, North-Holland, New York.

Thomas,P.D. & Middlecoff,J.F.,1980, Direct control of the grid point distribution in meshes generated by elliptic equations, AIAA Journal, Vol.18, No.6, pp.652-656.

Warming,R.F. & Beam,R.M.,1979, An extension of A-stability alternating direction implicit methods, BIT,19, pp.395-417.

Fig.1 Grid for the chilled pipeline, generated by equally spaced boundary values.

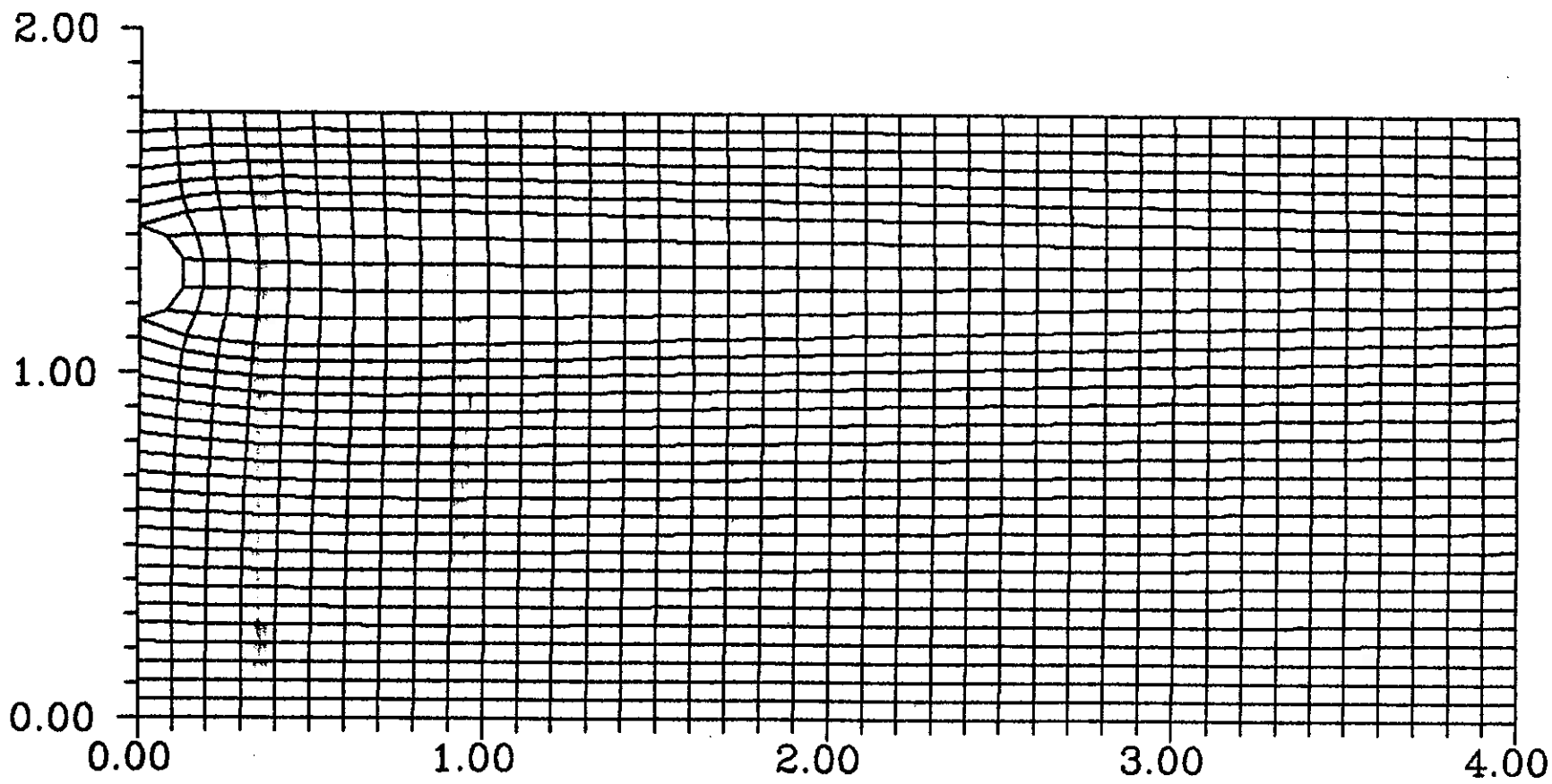

Fig.2 Grid for the chilled pipeline, generated by exponentially spaced boundary values.

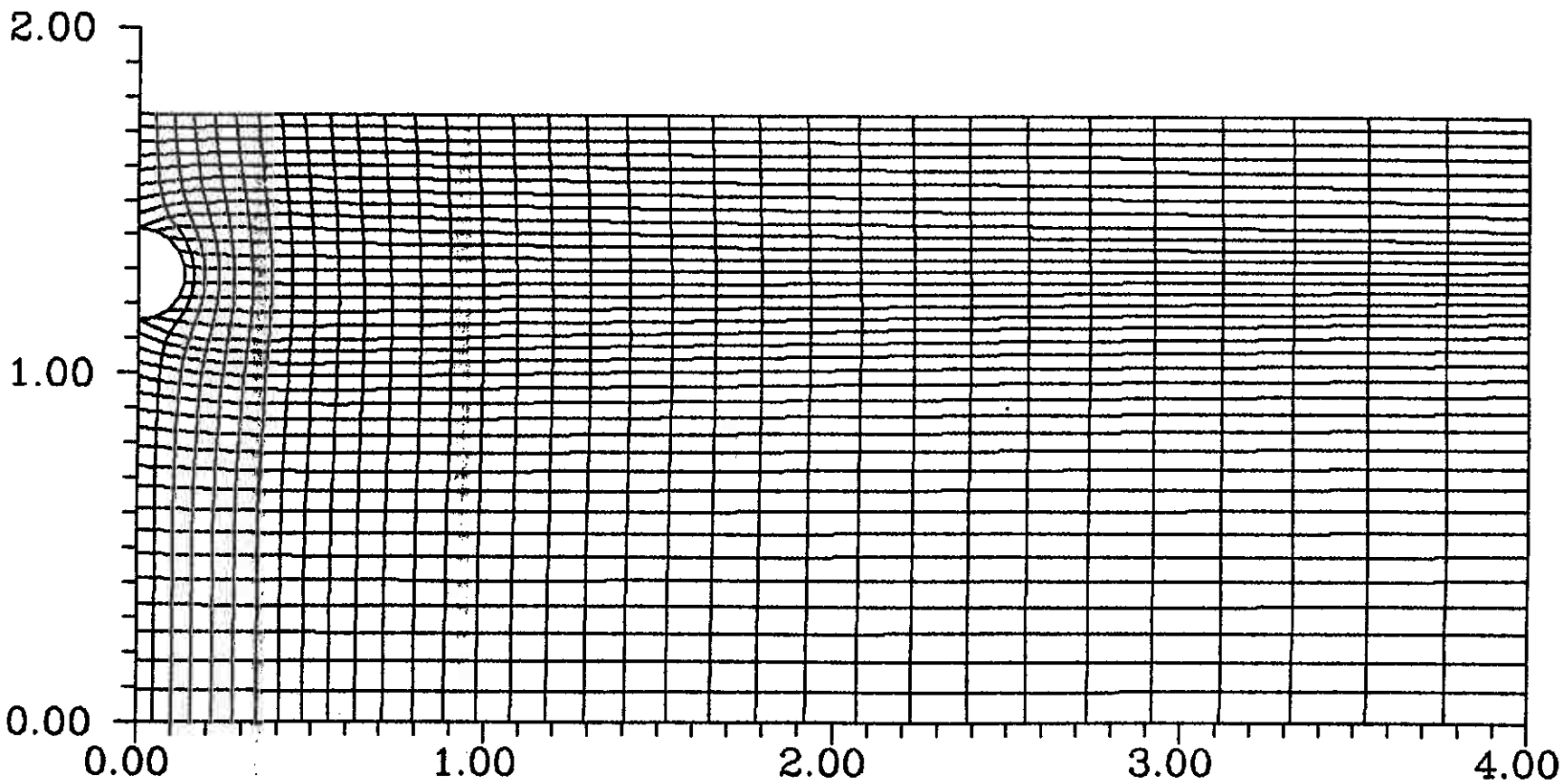

Appendix II

Density-Water Content Profiles

Water Contents Along Pipe Axis

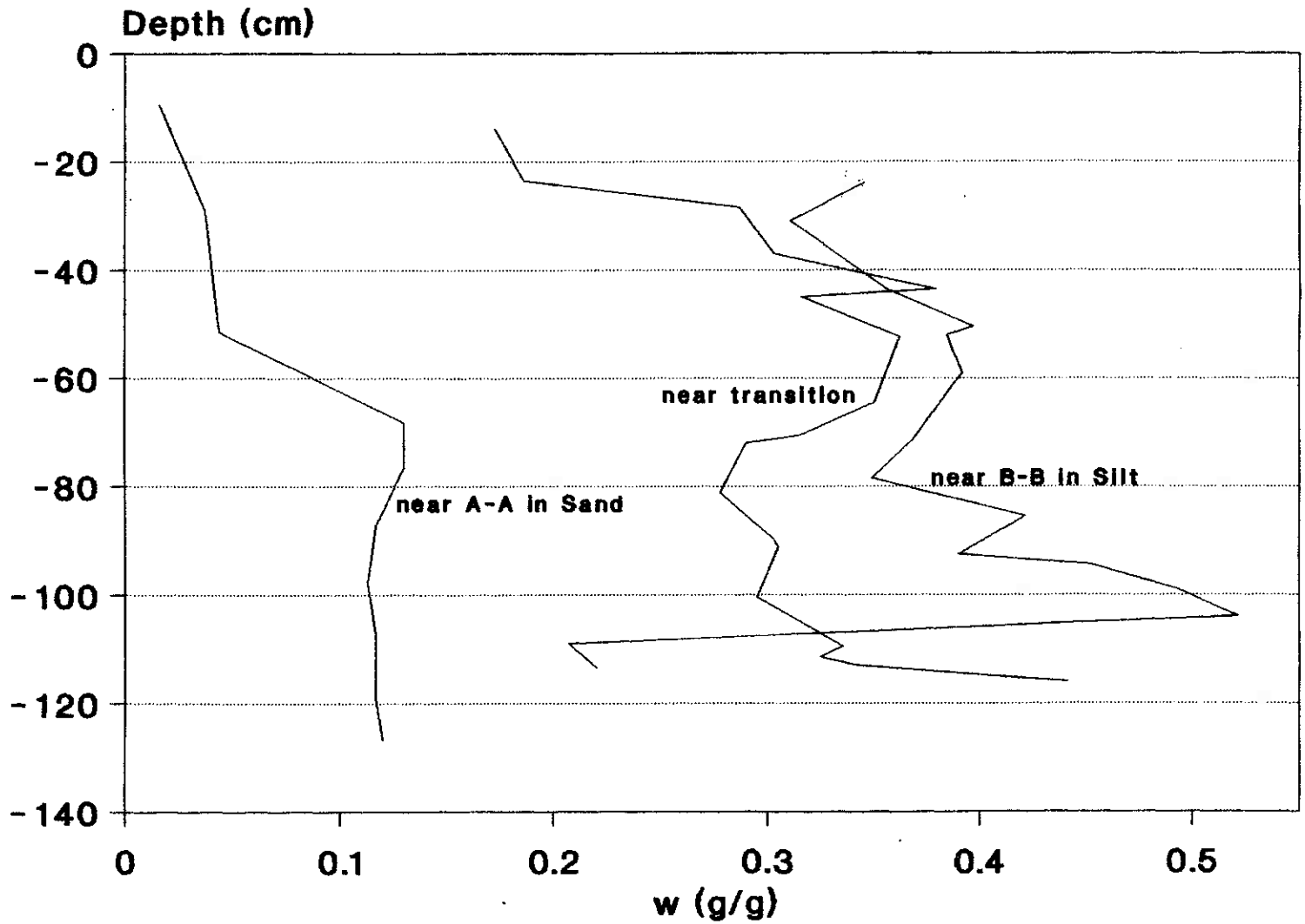

Water Contents Near Sand-Silt Transition

4th Freeze

22 cm off pipe axis

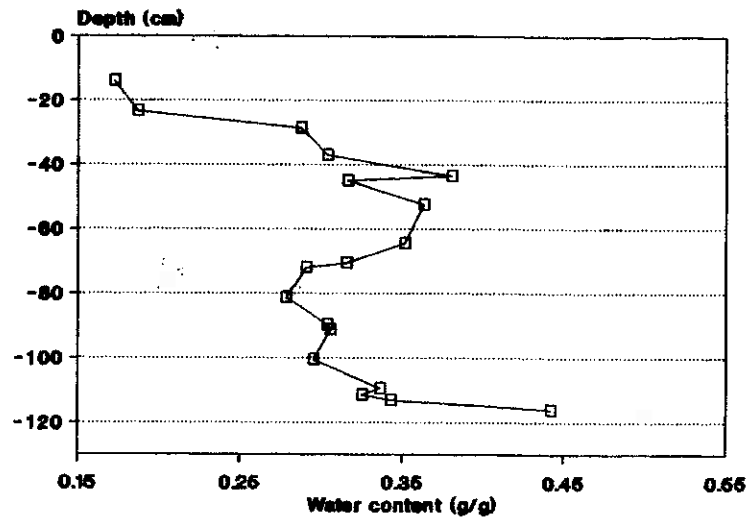

58 cm off pipe axis

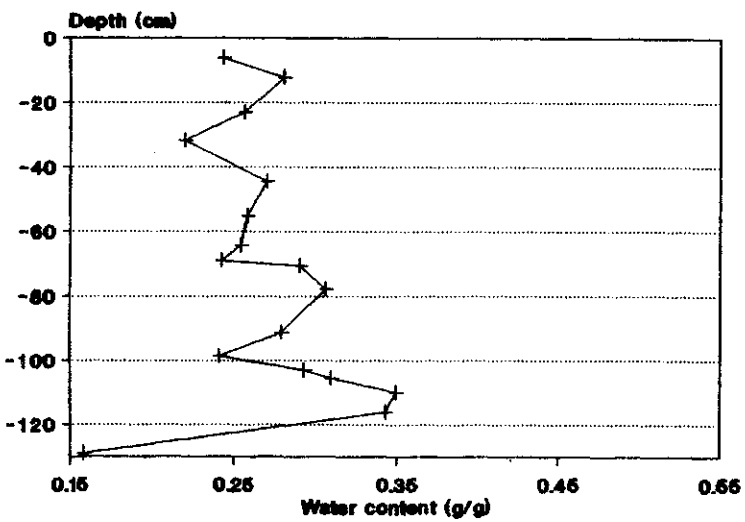

135 and 295 cm off pipe axis

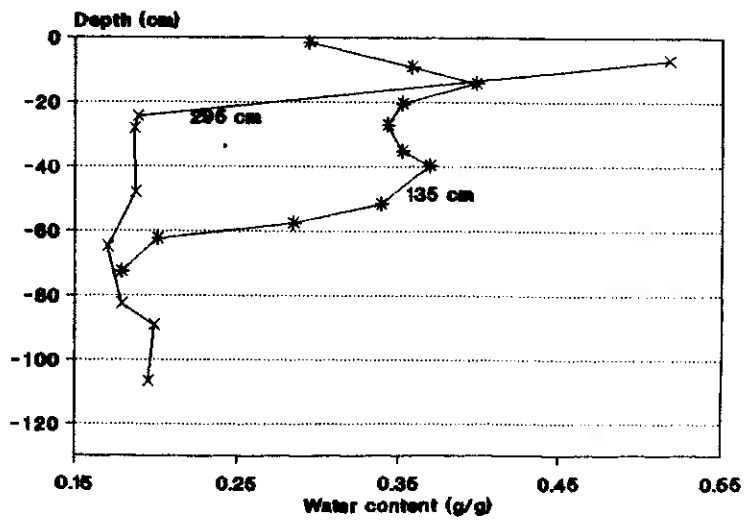

Water Contents at B-B Cross-section

4th Freeze

35 cm off pipe axis

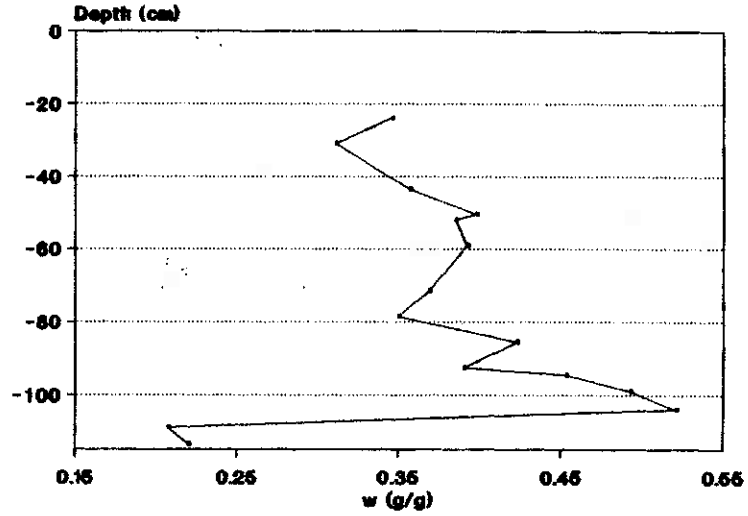

83 cm off pipe axis

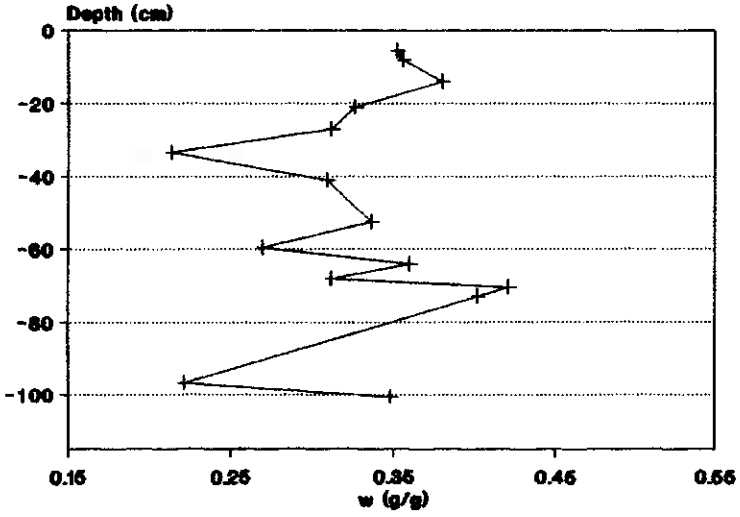
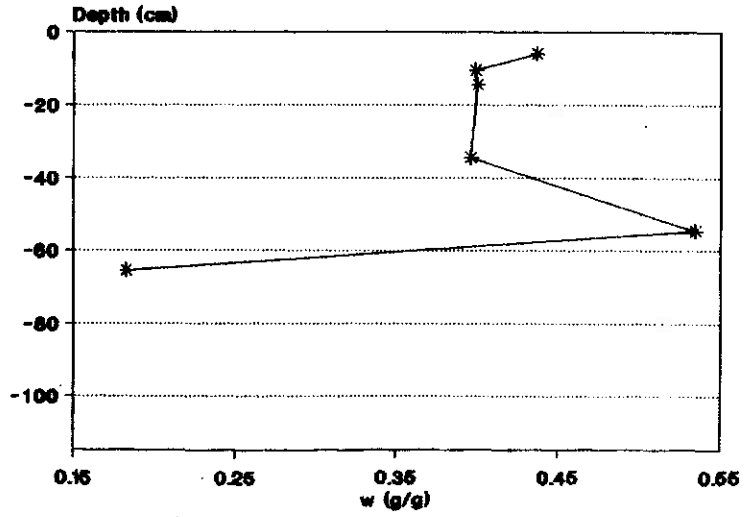
135 cm off pipe axis